

**Characteristics of atmospheric
turbulence near the ground
Part II: single point data for strong winds
(neutral atmosphere)**

Associated software: ESDUpac A9232 (Item No. 92032)

ESDU DATA ITEMS

Data Items provide validated information in engineering design and analysis for use by, or under the supervision of, professionally qualified engineers. The data are founded on an evaluation of all the relevant information, both published and unpublished, and are invariably supported by original work of ESDU staff engineers or consultants. The whole process is subject to independent review for which crucial support is provided by industrial companies, government research laboratories, universities and others from around the world through the participation of some of their leading experts on ESDU Technical Committees. This process ensures that the results of much valuable work (theoretical, experimental and operational), which may not be widely available or in a readily usable form, can be communicated concisely and accurately to the engineering community.

We are constantly striving to develop new work and review data already issued. Any comments arising out of your use of our data, or any suggestions for new topics or information that might lead to improvements, will help us to provide a better service.

THE PREPARATION OF THIS DATA ITEM

The work on this particular Data Item was monitored and guided by the Wind Engineering Panel. This Panel, which took over the work on wind engineering previously monitored by the Fluid Mechanics Steering Group, first met in 1979 and now has the following membership:

Chairman	
Mr T.V. Lawson	— Bristol University
Members	
Mr A. Allsop	— Ove Arup and Partners
Mr C.W. Brown	— Independent
Prof. J.E. Cermak*	— Colorado State University, USA
Dr N.J. Cook	— Building Research Establishment
Prof. A.G. Davenport*	— University of Western Ontario, Canada
Dr D.M. Deaves	— Atkins Research and Development
Dr R.G.J. Flay*	— University of Auckland, New Zealand
Dr A.R. Flint	— Flint and Neill
Mr R.I. Harris	— Cranfield Institute of Technology
Dr J.D. Holmes*	— CSIRO, Australia
Prof. K.C. Mehta*	— Inst. of Disaster Research, Texas Tech. Univ., USA
Mr R.H. Melling	— Independent
Dr W. Moores	— Meteorological Office, UK
Dr G.A. Mowatt	— Earl and Wright Ltd
Mr J.R.C. Pedersen	— Independent
Mr R.E. Whitbread	— BMT Fluid Mechanics Ltd
Mr G. Wiskin	— British Broadcasting Corporation.

* Corresponding Member

The technical work involved in the assessment of the available information and the construction and subsequent development of the Data Item was undertaken by

Mr N. Thompson — Head of Wind Engineering Group.

The person with overall responsibility for the work in this subject area is Mr N. Thompson, Head of Wind Engineering Group.

CHARACTERISTICS OF ATMOSPHERIC TURBULENCE NEAR THE GROUND PART II: SINGLE POINT DATA FOR STRONG WINDS (NEUTRAL ATMOSPHERE)

CONTENTS

	Page
1. NOTATION AND UNITS	1
2. PURPOSE, SCOPE AND APPLICABILITY OF THIS ITEM	3
3. INPUT DATA	4
4. TURBULENCE INTENSITIES AND REYNOLDS STRESSES	5
4.1 Turbulence Intensity: u -component	5
4.2 Turbulence Intensities: v - and w -components	5
4.3 Reynolds Stresses	6
5. PROBABILITY DENSITY	7
6. SPECTRAL DENSITY (UNIFORM TERRAIN)	8
6.1 Longitudinal u -component: High Frequency Range	8
6.2 Lateral v - and w -components: High Frequency Range	9
7. INTEGRAL LENGTH SCALES (UNIFORM TERRAIN)	10
7.1 Integral Length Scale; xL_u	10
7.2 Integral Length Scales; $^xL_v, ^xL_w$	10
8. NON-UNIFORM TERRAIN	11
8.1 Effect of Roughness Changes on xL_u and S_{uu}	11
9. UNCERTAINTIES	12
9.1 Turbulence Intensity	12
9.2 Spectral Density	12
10. REFERENCES AND DERIVATION	13
10.1 References	13
10.2 Derivation	13
 APPENDIX A NOTES ON THE BASIS OF THE HIGH FREQUENCY SPECTRAL DATA AND LENGTH SCALES	
A1. ADDITIONAL NOTATION	20
A2. DERIVATION OF SPECTRA AND LENGTH SCALES (EQUILIBRIUM BOUNDARY LAYER)	20
A2.1 Von Karman Model	20

A2.2	Kolmogorov Spectral Density Model	21
A3.	NON-EQUILIBRIUM BOUNDARY LAYER	24
A3.1	Equations for Calculating Local Values of $[^xL_u]_x$ for Single Roughness Change	25
A3.2	Multiple Roughness Changes	27
A3.3	Comparison With Measured Data	27
A4.	ADDITIONAL REFERENCES	27
APPENDIX B MODIFIED VON KARMAN SPECTRAL EQUATIONS (AND AUTOCORRELATION FUNCTIONS) FOR COMPLETE FREQUENCY RANGE		
B1.	ADDITIONAL NOTATION	28
B2.	BACKGROUND	28
B3.	MODIFIED EQUATIONS FOR AUTOCORRELATION FUNCTIONS	29
B3.1	Simplified Equations for the Autocorrelation Functions	30
B4.	MODIFIED EQUATIONS FOR SPECTRAL DENSITY FUNCTIONS	31
B5.	EXPRESSIONS FOR α , β_1 AND β_2	32
B6.	ADDITIONAL REFERENCE	33

CHARACTERISTICS OF ATMOSPHERIC TURBULENCE NEAR THE GROUND

Part II: single point data for strong winds (neutral atmosphere)

1. NOTATION AND UNITS

		<i>Units</i>	
		<i>SI</i>	<i>British</i>
d	effective displacement height of zero-plane above ground due to surrounding obstacles (Section 3)	m	ft
c	exponent in expression giving k_L		
f	Coriolis parameter ($f = 2\Omega \sin \phi$)	rad/s	rad/s
h	boundary layer height ($h = u_*/(6f)$)	m	ft
I_i	intensity of turbulence ($I_i = \sigma_i/V_z$)		
i	general values of u - , v - or w -component at point in space at time t ($i = u, v$ or w)	m/s	ft/s
j	number of roughness changes between site and upwind equilibrium conditions (see Sketch 8.1)		
k_L	factor accounting for variation of xL_u with V_{10r} and f (Figure 3b)		
$^xL_u, ^xL_v, ^xL_w$	length scales of turbulence in x -direction relating to u - , v - and w -components respectively	m	ft
n	frequency	Hz	Hz
n_i	$^xL_i n / V_z$		
P_i	cumulative probability that any value of i will be less than a particular value, i_p		
p_i	probability density functions of u - , v - or w -component	s/m	s/ft
S_{uu}, S_{vv}, S_{ww}	spectral density functions of u , v - and w -components respectively ($0 < n < \infty$)	m ² /s	ft ² /s
T	averaging time or response period of measuring instrument	s	s
T_0	duration of sample or wind-speed record	s	s
t	time	s	s

u_*	friction velocity [$u_* = V_{10}/(2.5 \ln(10/z_0))$]	m/s	ft/s
u, v, w	fluctuating components of wind speed at time t along x -, y - and z -axes respectively	m/s	ft/s
V_{10r}	reference hourly-mean wind speed at $z = 10$ m for terrain with $z_0 = 0.03$ m	m/s	ft/s
V_h	gradient wind speed at $z = h$	m/s	ft/s
V_z	hourly-mean wind speed at height z	m/s	ft/s
x	distance of terrain roughness change upwind of site	m	ft
x, y, z	system of rectangular Cartesian co-ordinates with x -axis defined in direction of mean wind	m	ft
z	height above zero plane (see Section 3)	m	ft
z_0	surface roughness parameter (see Section 3)	m	ft
z_b, z_t	height of inner and outer layers respectively of non-equilibrium boundary layer (see Sketch 8.1)	m	ft
ϕ	angle of latitude at site	degree	degree
ρ	air density	kg/m ³	slug/ft ³
σ_i	standard deviation of i -component at height z for $T \rightarrow 0$ and $T_0 \rightarrow \infty$; $\sigma_i = \overline{(i^2)}^{1/2}$	m/s	ft/s
$\sigma_i\{T, T_0\}$	standard deviation of i -component corresponding to finite T and T_0	m/s	ft/s
τ	time lag	s	s
τ_z	shear stress	kN/m ²	lbf/ft ²
Ω	angular rotation of Earth ($= 72.9 \times 10^{-6}$ rad/s)	rad/s	rad/s
Subscripts			
b	relates to value at inner layer of atmospheric boundary layer (see Sketch 8.1)		
j	relates to value for upwind equilibrium conditions (upwind of j^{th} roughness change)		
x	relates to site value when roughness changes exist upwind (non-equilibrium conditions)		
A bar ($\bar{}$)	denotes time-averaged values		
A prime (\prime)	indicates value for $V_{10r} = 20$ m/s		

2. PURPOSE, SCOPE AND APPLICABILITY OF THIS ITEM

Turbulence data are required for engineering calculations of gust speeds (see ESDU 83045⁶) and mean and fluctuating loading. In particular, spectral densities are required as input data for methods used in assessing dynamic response.

The definition of the properties described in this Item and other background information are given in Reference 3. The purpose of this Item, which supersedes ESDU 74031, is to provide the statistical properties of turbulence in the atmospheric boundary layer at a single point in space. The properties of turbulence at two points in space are dealt with in Reference 4.

In this Item the properties considered are:

- (i) intensities and Reynolds stresses,
- (ii) probability densities,
- (iii) spectral densities and integral length scales of turbulence.

The statistical properties presented are derived from world-wide measurements in the atmospheric boundary layer and, within the uncertainties of the data, can be taken to apply for neutral atmosphere* conditions which include strong winds ($V_{10} > 10$ m/s).

The data are mainly based on measured values for homogeneous terrain (*e.g.* open country or forests) but some measurements are available for built-up areas and these indicate that, within the scatter of the data, the present model is applicable for heights greater than about 10 m above the general level of ground obstructions. When the upwind fetch of uniform terrain is less than about 30 km the effect of roughness changes should be considered (see Section 8).

For very hilly or mountainous terrain the spectral data in Section 6 do not apply. In such cases secondary peaks in the normalised spectra (nS_{ii}/σ_i^2) may occur at low frequencies (see, for example, Derivation 27). Some additional data for complex terrain are provided in Derivation 44.

The principal difference between the data presented in this Item and previous data (for example in ESDU 74031 which this Item supersedes) is that this Item recognises that the characteristic properties of turbulence (variances and length scales) are dependent on wind speed (except in a layer close to ground level). The reason for this is that the present data are based on similarity theory which shows that as the reference wind speed increases, the boundary layer depth increases and the typical size and intensity of turbulence within the boundary layer are then scaled accordingly.

Sections 3 to 7 present the data for uniform terrain (equilibrium boundary layer) conditions. Section 8 provides guidance on the effect of step changes in terrain roughness upwind of the site. Section 9 discusses the uncertainty of the data. The Appendices contain the equations from which the graphical data are obtained and gives the background to their derivation and to the methods given in the main part of the Item.

The full methods on which this Data Item is based have been programmed into the software package, ESDUpac A9232, described in ESDU 92032¹⁰.

* See Item 82026⁵ for a further explanation of this term and its applicability to the strong wind condition.

3. INPUT DATA

A description of the atmospheric boundary layer and the mechanisms producing turbulence are contained in Item 74030³. The main factors that affect turbulence in the neutral atmospheric boundary layer (and hence the parameters that are required as input data when using this Item) are:

- (i) surface roughness parameter, z_0 , see Table 3.1,
- (ii) the height above the zero plane (see following),
- (iii) hourly-mean reference wind speed (V_{10r}) and the local hourly-mean wind speed.

The relationship between V_{10r} and V_{10} and the variation of mean wind speed, V_z , with height and terrain roughness (including terrain with roughness changes) is dealt with in ESDU 82026⁵ and 84011⁷ and the user should refer to those documents for data appropriate to strong-wind or neutral atmosphere conditions, or, preferably, use the computer program ESDUpac A9232 described in ESDU 92032¹⁰.

The height, z , at which the properties are presented is measured from the zero-plane displacement height, d , above the ground, so that height above ground is given by $(z + d)$. Approximate values of d are given in Table 3.1 based on the assumption that the zero-plane is about one or two metres below the general height of the surrounding buildings or trees. For more detailed information see ESDU 82026⁵.

TABLE 3.1 Typical Values of Terrain Parameters z_0 and d

Terrain Description	z_0 (m)	d (m)
City centres Forests	0.7	15 to 25
Small towns Suburbs of large towns and cities Wooded country (many trees)	0.3	5 to 10
Outskirts of small towns Villages Countryside with many hedges, some trees and some buildings	0.1	0 to 2
Open level country with few trees and hedges and isolated buildings; typical farmland	0.03	0
Fairly level grass plains with isolated trees	0.01	0
Very rough sea in extreme storms (once in 50-yr extreme) Flat areas with short grass and no obstructions Runway area of airports	0.003	0
Rough sea in annual extreme storms Snow covered farmland Flat desert or arid areas Inland lakes in extreme storms	0.001	0

4. TURBULENCE INTENSITIES AND REYNOLDS STRESSES

4.1 Turbulence Intensity: u -component

Turbulence intensity is a measure of the magnitude of the fluctuating velocity component compared to the hourly-mean wind speed at the same height. It is a non-dimensional quantity derived from the variance (σ_i^2) and for the u -component is $I_u = \sigma_u/V_z$.

For the situation where the terrain is uniform upwind of the site for at least 30 km (*i.e.* the atmospheric boundary layer is in dynamic equilibrium with the underlying surface) values of I_u are given by Equations (4.1) to (4.3). The derivation of these data is summarised in Item 83045 and a simplified presentation is given in Figure 1. Figure 1a provides values of I_u' when the reference wind speed (V_{10r}) is 20 m/s. Figure 1b gives a correction factor by which I_u' must be multiplied when $V_{10r} \neq 20$ m/s.

$$I_u = \frac{\sigma_u}{u_*} \frac{u_*}{V_z} \quad (4.1)$$

where

$$\frac{\sigma_u}{u_*} = \frac{7.5\eta[0.538 + 0.09 \ln(z/z_0)]^p}{1 + 0.156 \ln(u_*/(fz_0))} \quad (4.2)$$

$$\eta = 1 - 6fz/u_* ; p = \eta^{16}$$

and

$$V_z/u_* = 2.5[\ln(z/z_0) + 34.5fz/u_*]. \quad (4.3)$$

For the situation where there are roughness changes upwind of the site within $x = 30$ km the local intensity of turbulence, I_{ux} , will deviate from the equilibrium value increasingly as x decreases. A simplified method for estimating I_{ux} , for a site with up to two step changes in terrain roughness upwind, is provided in Item 84030⁸. The results are presented in tabular form and approximate correction factors for hilly terrain are also provided. Item 92032¹⁰ also contains a computer program to evaluate I_{ux} for flat or hilly terrain.

4.2 Turbulence Intensities: v - and w -components

Data from sources where both σ_u and σ_v , or σ_u and σ_w , have been measured simultaneously for neutral atmospheric conditions indicate that near the ground the ratios σ_v/σ_u and σ_w/σ_u are essentially constant irrespective of the nature of the terrain. Thus, values of I_v and I_w (and I_{vx} and I_{wx}) can be obtained by evaluating I_u (or I_{ux} if roughness changes are to be considered) for the site in question and then multiplying this value by the ratio σ_v/σ_u or σ_w/σ_u (Figure 2). These are represented by

$$\frac{\sigma_v}{\sigma_u} = 1 - 0.22 \cos^4\left(\frac{\pi z}{2h}\right) \quad (4.4)$$

and

$$\frac{\sigma_w}{\sigma_u} = 1 - 0.45 \cos^4\left(\frac{\pi z}{2h}\right) \quad (4.5)$$

where h can be taken as $u_*/(6f)$.

This procedure assumes that the effect of any upwind roughness changes on σ_v and σ_w can be accounted for, to a first approximation, through the effect on the u -component. At large heights above the ground, as $z \rightarrow h$, σ_v/σ_u , and σ_w/σ_u both tend to unity.

4.3 Reynolds Stresses

Retarding forces exerted on the wind at the surface of the Earth are transmitted upwards through the atmospheric boundary layer by shear forces, called Reynolds stresses, and also by the exchange of momentum, due to the movement of air. In applications to wind loading on ground-based structures knowledge of the Reynolds stresses is only required in special cases.

The Reynolds stresses are obtained from the co-variances \overline{uv} , \overline{vw} and \overline{uw} and are zero for isotropic* turbulence. Near the ground surface friction distorts the symmetry of turbulence and non-isotropic conditions result. However, in practice, the co-variances \overline{uv} and \overline{vw} are small and can be ignored but this is not so for the \overline{uw} co-variance.

The co-variance \overline{uw} is defined by the shear stress,

$$\tau_z = -\rho \overline{uw} = \rho u_*^2 (1 - z/h)^2. \quad (4.6)$$

Thus for heights up to about 300 m

$$\frac{-\overline{uw}}{\sigma_u \sigma_w} \approx \frac{u_*^2 (1 - 2z/h)}{\sigma_u (\sigma_w/\sigma_u) \sigma_u} = \frac{1 - 2z/h}{(\sigma_u/u_*)^2 (\sigma_w/\sigma_u)} \quad (4.7)$$

where, for an equilibrium boundary layer, σ_u/u_* is given by Equation (4.2) and $\sigma_w/\sigma_u \approx 0.55$ (Figure 2).

Reported values of $-\overline{uw}/(\sigma_u/\sigma_w)$ in the literature tend to be slightly higher than values given by Equation (4.7). The probable reason is the response characteristics of typical anemometers used to measure the vertical component of wind speed.

* For isotropic turbulence the statistical properties do not change when the reference co-ordinates are rotated, *i.e.*, the properties are independent of direction in the turbulence field.

5. PROBABILITY DENSITY

This property describes how the magnitudes of the fluctuating velocity components are distributed. A common assumption, which is reasonable in many applications, is that atmospheric turbulence is a ‘normal’ or Gaussian process with a probability density function for which

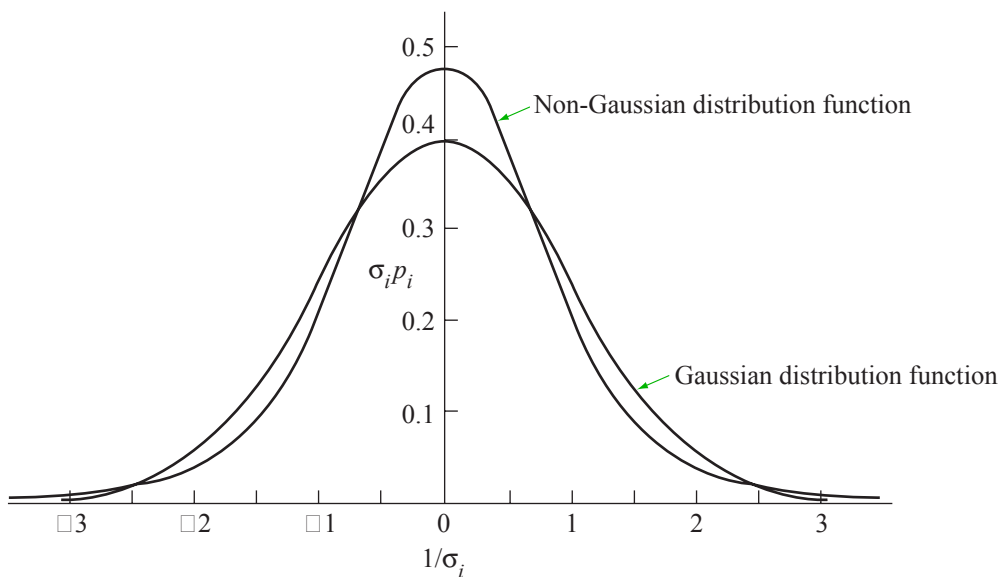
$$p_i = \frac{1}{\sigma_i(2\pi)^{1/2}} \exp[-i^2/2\sigma_i^2] \quad (5.1)$$

where $i = u, v$ or w . The integral

$$P_i = \int_{-\infty}^{i_p} p_i di \quad (5.2)$$

gives the proportion of all values which can be expected to have values below a particular value i_p .

In practice, atmospheric turbulence contains “patches” of a significantly non-Gaussian nature (particularly in the lower 30 m) when larger gusts and longer lulls may occur more frequently than indicated by the Gaussian distribution, as illustrated in Sketch 5.1.



Sketch 5.1 Probability density function

For the calculation of wind loads on, and the response of, buildings in strong winds it is generally satisfactory in most applications to assume that the probability distribution is Gaussian. In the calculation or simulation of aircraft response to atmospheric turbulence this is not necessarily so and there have been several attempts to develop non-Gaussian models that are applicable to the “patches” mentioned earlier. One method is to generate a non-Gaussian random process by the multiplication of two Gaussian processes (see Reference 1). An alternative is to represent wind fluctuations as a statistical aggregate of “discrete gusts” (see Reference 2).

6. SPECTRAL DENSITY (UNIFORM TERRAIN)

As explained more fully in Reference 3, the variance (σ_i^2) of a fluctuating component is made up from contributions over a range of frequencies; the spectral density property describes this frequency distribution and is particularly important in assessing dynamic effects induced by the wind at or near a natural frequency of a structure.

Considerable numbers of measurements of the spectra of gust velocities in the near-neutral atmosphere, or strong wind condition, at varying heights and for different terrains are available. Many of these show wide variations from each other when plotted in normalised form (e.g. nS_{ii}/σ_i^2 against $\ln n$), particularly in the low frequency region.

It is possible to attribute some of these variations to non-equilibrium boundary layer effects due to changes in terrain roughness upwind of, and close to, the measuring site and also to measuring and processing techniques. Methods of allowing for the effects of non-uniform terrain are given in Section 8. Also non-stationarity of the wind velocity measurements (when, in particular, the mean wind speed over successive intervals is varying with time) affects the form of the spectrum. However, the assumption of stationarity should lead to conservative loadings on conventional structures.

In most practical applications only spectral densities in the high frequency region are required and in this situation the data formulation can be considerably simplified. For simplicity of use, only the high frequency spectral data are given in Section 6.1. The forms of spectral equation applicable over the complete frequency range currently in use (e.g. the von Karman form) are not entirely satisfactory in representing measured data for all frequencies and heights in the atmospheric boundary layer. A modified von Karman model for spectral densities over the whole frequency range, together with the corresponding autocorrelation functions, is presented in Appendix B and is compatible with the high frequency data in Section 6.1.

6.1 Longitudinal u -component: High Frequency Range ($nz/V_z > 0.1$)

The von Karman spectral equations (Equations (A2.1) and (A2.2) in Appendix A) have been generally accepted as the best analytical representation of isotropic turbulence over the whole frequency range. The effect of departure from isotropic turbulence near the ground can be allowed for by the variation with height and surface roughness of the appropriate variance σ_i^2 and length scale parameter xL_i since they typify the intensity and size of eddies constituting turbulence. However, high quality measurements of the autocorrelation (ρ_{ii}) and spectral density (S_{ii}) functions have shown that the integral length scale parameter, as given by

$$^xL_i = V_z \int_0^\infty \rho_{ii} d\tau, \quad (6.1)$$

when used in the von Karman spectral equation gives underestimates of spectral density in the high frequency region. The von Karman equation is therefore inadequate in representing all the characteristic properties of turbulence although it reduces to the correct functional form in the high frequency range ($nz/V_z > 0.1$) when

$$\frac{nS_{uu}}{\sigma_u^2} = A \left(\frac{^xL_u n}{V_z} \right)^{2/3}. \quad (6.2)$$

In order to ensure that the integral length scale given by Equation (6.1) can be used directly in Equation (6.2)

to predict S_{uu} , it can be established (see Section A2.1 of Appendix A) that the parameter A is given by

$$A = 0.115 [1 + 0.3151(1 - z/h)^6]^{2/3} \quad (6.3)$$

and takes the von Karman value of 0.115 for large heights but increases to a value of 0.142 close to the ground. For values of xL_u , see Section 7.1.

6.2 Lateral v - and w -components: High Frequency Range ($nz/V_z > 0.1$)

For the v - and w -components, corresponding expressions for the spectral density in the high frequency range are given by

$$\frac{S_{vv}}{S_{uu}} = \frac{S_{ww}}{S_{uu}} = \frac{4}{3} \quad (6.4)$$

which is compatible with the von Karman expression in the high frequency range when the assumption of local isotropy is valid ($^xL_v = ^xL_w = \frac{1}{2} ^xL_u$).

7. INTEGRAL LENGTH SCALES (UNIFORM TERRAIN)

7.1 Integral Length Scale; xL_u

A relation for the integral length scale xL_u is derived in Section A2 of Appendix A and is given by Equation (A2.14) in Section A2.2.

The variation of xL_u with z and z_0 for a reference wind speed of $V_{10r} = 20$ m/s over open country terrain ($z_0 = 0.03$ m), and a value of the Coriolis parameter of $f = 1 \times 10^{-4}$ rad/s, is presented in Figure 3a. A simplified correction factor (k_L) accounting for the variation of xL_u with V_{10r} and f is presented in Figure 3b. The factor k_L is an approximation of the results obtained using Equation (A2.14) but in general will give agreement to within about $\pm 8\%$. The variation of xL_u with height, terrain roughness and wind speed depicted by Figure 3 is more complex than previous formulations because it is the result of a more realistic modelling of the physical processes occurring in the atmospheric boundary layer as described in the following paragraph.

Turbulence in the atmospheric wind originates from the action of the shear stress at ground level (due to surface roughness and ground obstructions) which is transmitted upwards through the atmosphere leading to the generation, and decay, of eddies. According to similarity theory, in a layer close to the ground the size of these eddies varies primarily with the degree of surface roughness (z_0) so that, at a fixed height above ground level, the eddy size is invariant with wind speed, and is smaller over a rougher surface (with larger z_0). For larger heights above ground level similarity theory predicts that the size of eddies is stretched in proportion to the depth (h) of the planetary boundary layer. Thus, at a fixed height in this region, the eddy size increases with increasing wind speed (V_{10r}) and is larger over a rougher surface in accordance with the known behaviour of h with V_{10r} and z_0 . In this context it is important to note that the model described in Section A2 of Appendix A reflects these trends.

Previous purely empirical formulations for xL_u have indicated the first trend because wind and turbulence records are often obtained at heights comparatively near the ground and at moderate hourly-mean wind speeds corresponding to $V_{10r} \approx 10$ m/s. Equivalent design wind speeds are more in the region of $V_{10r} = 20$ m/s to 30 m/s and the importance of the semi-theoretical basis of the model is that it lends confidence in extrapolating the measured data at moderate wind speeds (and moderate heights) to the much higher design wind speed case at heights corresponding to taller buildings for which dynamic effects are more significant. The result, for moderate- to high-rise buildings, is an overall decrease in dynamic response but a small increase in the non-resonant response due to turbulence buffeting.

7.2 Integral Length Scales; $^xL_v, ^xL_w$

It follows from the existence of isotropy in the high frequency region (Section 6.2) that the length scales xL_v and xL_w can be related directly to xL_u for the same wind and terrain conditions. These relations are

$$^xL_v/^xL_u = 0.5(\sigma_v/\sigma_u)^3, \quad (7.1)$$

and
$$^xL_w/^xL_u = 0.5(\sigma_w/\sigma_u)^3, \quad (7.2)$$

where (σ_v/σ_u) and (σ_w/σ_u) are given by Figure 2 and are represented by the empirical equations

$$\frac{\sigma_v}{\sigma_u} = 1 - 0.22 \cos^4 \left(\frac{\pi}{2} \frac{z}{h} \right) \quad (7.3)$$

and
$$\frac{\sigma_w}{\sigma_u} = 1 - 0.45 \cos^4 \left(\frac{\pi}{2} \frac{z}{h} \right). \quad (7.4)$$

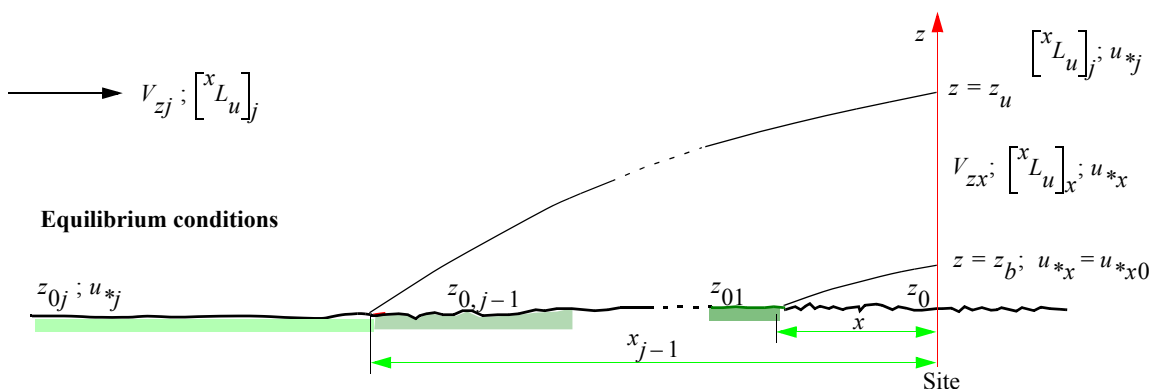
8. NON-UNIFORM TERRAIN

In practice it is exceptional that a sufficiently long upwind fetch of uniform terrain occurs for an equilibrium boundary layer to exist. The open sea, large plains and extensive forests which extend more than about 30 kilometres are examples where an equilibrium boundary layer can exist; in many countries, apart from stretches of fairly flat open country away from the coastal regions, this situation is unlikely. There may be several changes in the upwind terrain roughness within a few kilometres of the site in question; the variation of wind speed and turbulence with height is then no longer independent of the fetch, x .

Items 82026⁵, 83045⁶ and 84030⁸ provide simplified methods for estimating the effects of upwind roughness changes on the variation with height of mean wind and gust speed as well as longitudinal turbulence intensity. The factors provided by these methods can be extended to lateral and vertical turbulence intensities through Equations (4.4) and (4.5). These data are based on the methods of Deaves^{41, 42} for a single roughness change, extended to cater for multiple roughness changes (and hill effects). No definitive method exists for calculating the effects of roughness changes on integral length scale or spectral density but the approach summarised in Section A3.1 of Appendix A is suggested as a means of providing an estimate for a single roughness change and as a more tentative method for multiple roughness changes.

8.1 Effect of Roughness Changes on xL_u and S_{uu}

For a site with a single smooth-to-rough change (*i.e.* $z_0 > z_{01}$) a distance x upwind of the site, the length scale at the site will be smaller than the corresponding value for the site terrain when $x > 50$ km (approximately equilibrium conditions). The reverse situation occurs when the change is from rough to smoother terrain. As z increases, the length scale will tend towards the corresponding equilibrium value for the upwind terrain (z_{01}) at the same height. When there are other intermediate roughness changes the situation is more complicated but the same overall trends are to be expected.



Sketch 8.1

The method described in Section A3.1 is most appropriate when dealing with a single roughness change upwind of the site. When applied to the situation where multiple roughness changes occur the results are more tentative.

The method is not suitable for hand calculations. However, in Item 86035⁹ tables of integral length scale are presented for sites with various upwind changes in terrain roughness. These tables are based on the method described in Section A3.1 of Appendix A. The corresponding spectral density values follow from using Equation (6.2) with $^xL_{ux}$, V_{zx} and σ_{ux} substituted for xL_u , V_z and σ_u . Values of I_{ux} ($= \sigma_{ux}/V_{zx}$) and V_{zx} can be obtained from the tables in Items 84030⁸ and 84011⁷ respectively. Also, the computer

program in Item 92032¹⁰ can be used for sites with multiple roughness changes upwind to calculate integral length scales of turbulence, as well as wind speed and turbulence intensity profiles, for the u -, v - and w -components.

9. UNCERTAINTIES

9.1 Turbulence Intensity

The experimental data used to derive Equation (4.2) for the u -component suggests an uncertainty of about $\pm 10\%$ for equilibrium conditions (x greater than about 30 km). For non-uniform terrain a larger uncertainty of $\pm 20\%$ should be allowed. Similar uncertainties are likely to apply for the v - and w -components.

9.2 Spectral Density

It is difficult to assess precisely the accuracy of the spectral data presented because of the varying techniques and methods of analysis used to derive the data in the various sources. In the high frequency range ($nz/V_z > 0.1$) good quality data suggest that the uncertainty for the u -component under equilibrium conditions ($x > 30$ km) is approximately $\pm 20\%$. However, in situations where the mean wind conditions are not constant over the period of observation, or where the upwind terrain is not uniform (see also Section A3.3 of Appendix A), this uncertainty will increase to about $\pm 30\%$.

The departures are more marked at heights below about 30 m and at low frequencies when turbulence becomes more and more anisotropic. In particular, data for the w -component are affected by the presence of the ground when the energy in large eddies (*i.e.* at low frequencies) is transferred to the u - and v -components.

The estimated spectral data for rough terrain, such as built-up areas, cannot be assessed properly because of the lack of sufficient reliable measurements but it is important in this case that the effect of upwind changes in terrain are taken into account.

There are few reliable spectral measurements for the v - and w -components in strong winds on which to assess the uncertainties of the present data but they are likely to be of the same order as for the u -component.

10. REFERENCES AND DERIVATION

10.1 References

The References given are recommended sources of information supplementary to that in this Data Item.

1. REEVES, P.M. A non-Gaussian turbulence simulation. Air Force Flight Dynamics Lab. Rep. AFFDL-TR-69-67, 1969.
2. JONES, J.G. Statistical discrete-gust theory for aircraft loads. A progress report. RAE Tech. Rep. 73167, 1973.
3. ESDU Characteristics of atmospheric turbulence near the ground. Part 1: definitions and general information. Item No. 74030, ESDU International, London, 1974.
4. ESDU Characteristics of atmospheric turbulence near the ground. Part III: variations in space and time for strong winds (neutral atmosphere). Item No. 86010, ESDU International, London, 1986.
5. ESDU Strong winds in the atmospheric boundary layer. Part 1: mean-hourly wind speeds. Item No. 82026, ESDU International, London, 1982.
6. ESDU Strong winds in the atmospheric boundary layer. Part 2: discrete gust speeds. Item No. 83045, ESDU International, London, 1983.
7. ESDU Wind speed profiles over terrain with roughness changes for flat or hilly sites. Item No. 84011, ESDU International, London, 1984.
8. ESDU Longitudinal turbulence intensities over terrain with roughness changes. Item No. 84030, ESDU International, London, 1984.
9. ESDU Integral length scales of turbulence over flat terrain with roughness changes. Item No. 86035, ESDU International, London, 1986.
10. ESDU Computer program for wind speeds and turbulence properties: flat or hilly sites in terrain with roughness changes. Item No. 92032 and program A9232 (on disk in Vol. S/W1), ESDU International, 1992.

10.2 Derivation

The Derivation lists selected sources that have assisted in the preparation of this Data Item.

11. PANOFSKY, H.A.
McCORMICK, R.A. The spectrum of vertical velocity near the surface. Inst. Aero. Sci., Rep. 59-6, 1959.
12. DAVENPORT, A.G. The spectrum of horizontal gustiness near the ground in high winds. *Q. J. R. Met. Soc.*, Vol. 87, pp. 194-211, April 1961.
13. SOMA, S. The properties of atmospheric turbulence in high winds. *J. Met. Soc. Japan*, Vol. 42, pp. 372-396, 1964.

14. BERMAN, S. Estimating the longitudinal wind spectrum near the ground. *Q. J. R. Met. Soc.*, Vol. 91, pp. 302-317, July 1965.
15. BUSCH, N.E.
PANOFSKY, H.A. Recent spectra of atmospheric turbulence. *Q. J. R. Met. Soc.*, Vol. 94, pp. 132-148, April 1968.
16. CASE, E.R.
MARITAN, P.A.
GORJUP, M. Development of a low altitude gust model and its application to STOL aircraft response studies. De Havilland Aircraft of Canada Rep. DHC-DIR 68-15, May 1969.
17. SLADE, D.H. Wind measurement on a tall tower in rough and inhomogeneous terrain. *J. App. Met.*, Vol. 8, No. 2, pp. 293-297, April 1969.
18. FICHTL, G.H.
McVEHIL, G.E. Longitudinal and lateral spectra of turbulence in the atmospheric boundary layer. Paper No. 6, AGARD Conf. Proc. 48, February 1970.
19. COUNIHAN, J. A method of simulating a neutral atmospheric boundary layer in a wind tunnel. Paper No. 14, AGARD Conf. Proc. 48, February 1970.
20. CAMPBELL, G.S.
HANSEN, F.V.
DISE, R.A. Turbulence data derived from measurements on the 32-meter tower facility: White Sands missile range, New Mexico. U.S. Army Tech. Rep. ECOM-5314 (AD 711852), July 1970.
21. PANOFSKY, H.A.
MAZZOLA, C.A.
et al. Turbulence characteristics over heterogeneous terrain. U.S. Army Tech. Rep. ECOM-0079-F (AD 716361), September 1970.
22. TEUNISSEN, H.W. Characteristics of the mean wind and turbulence in the planetary boundary layer. Univ. of Toronto, Rev. 32, October 1970.
23. SITARAMAN, V. Spectra and cospectra of turbulence in the atmospheric surface layer. *Q. J. R. Met. Soc.*, Vol. 96, pp. 744-749, October 1970.
24. BOWNE, N.E.
BALL, J.T. Observational comparison of rural and urban boundary layer turbulence. *J. App. Met.*, Vol. 9, pp. 750-775, October 1970.
25. ADELFGANG, S.I. Standard deviation of turbulence velocity components over flat arid terrain. *J. Geophys. Res.*, Vol. 75, pp. 6864-6867, November 1970.
26. SHIOTANI, M. Structure of gusts in high winds. Nihon University, Japan, Physical Sci. Lab. Interim Report, Parts 2-5, 1968-1971.
27. PANOFSKY, H.A. Variances and spectra of vertical velocity just above the surface layer. *Boundary-layer Met.*, Vol. 2, pp. 30-37, September 1971.
28. COLMER, M.J. Measurements of horizontal wind speed and gustiness made at several levels on a 30 m mast. RAE Tech. Rep. 71214, November 1971.
29. IZUMI, Y. Kansas 1968 field program data report. Air Force Cambridge Res. Lab., Bedford, USA., Rep. AFCRL-72-0041, December 1971.
30. BROOK, R.R. The measurement of turbulence in a city environment. *J. App. Met.*, Vol. 11, pp. 443-450, April 1972.
31. HARRIS, R.I. Measurement of wind structure. Symposium on external flows, Bristol University, England, June 1972.

32. NAITO, G.
KONDO, J. Spatial structure of fluctuating components of the horizontal wind speed above the ocean. *J. Met. Soc. Japan*, Vol. 52, pp. 391-399, 1974.
33. DUCHENE-MARULLAZ, P. Structure fine du vent; premiers resultats. Internal rep., Centre Scientifique et Technique de Batiment, Nantes, France, January 1974.
34. DUCHENE-MARULLAZ, P. Turbulence atmospherique au voisinage d'une ville. C.S.T.B. En.N. Cli 75 - 2, Nantes, France, 1975.
35. HARRIS, R.I. Unpublished data for Rugby and Cranfield masts. Cranfield Institute of Technology, England.
36. EATON, K.J.
MAYNE, J.R. The measurement of wind pressure on two-storey houses at Aylesbury. *J. Indust. Aerodyn.*, Vol. 1 pp. 67-109, 1975.
37. PEARSE, R. The influence of two-dimensional hills on simulated atmospheric boundary layers. Ph.D Thesis, University of Canterbury, New Zealand, August 1978.
38. FLAY, R.G.J. Structure of a rural atmospheric boundary layer near the ground. Ph.D. Thesis, University of Canterbury, New Zealand, November 1978.
39. HARRIS, R.I.
DEAVES, D.M. The structure of strong winds. Paper 4 of CIRA Conf. on "Wind Engineering in the eighties", Construction Ind. Res. and Inf. Assoc., London 1980.
40. TEUNISSEN, H.W. Structure of mean wind and turbulence in the planetary boundary layer over rural terrain. *Boundary-layer Met.*, Vol. 19, pp. 187-221, 1980.
41. DEAVES, D.M. Computations of wind flow over changes in surface roughness. *J. Wind Engng Indust. Aerodyn.*, Vol. 7, pp. 65-94, 1981.
42. DEAVES, D.M. Terrain-dependence of longitudinal r.m.s. velocities in the neutral atmosphere. *J. Wind Engng Indust. Aerodyn.*, Vol. 8, pp. 259-274, 1981.
43. HANAFUSA, T.
FUJITANI, T. Characteristics of high winds observed from a 200 m meteorological tower at Tsukuba Science City. Papers in *Meteorology and Geophysics*, Vol. 32, pp. 19-35, 1981.
44. PANOFSKY, H.A. Spectra of velocity components over complex terrain. *Q. J. R. Met. Soc.*, Vol. 108, pp. 215-230, 1982.
45. WILLS, J.A.B.
COLE, L.R. Snorre dynamic wind study. BMT Project No. 25016, BMT Fluid Mechanics Ltd, Teddington, England, 1987.
46. MAEDA, J.
MAKINO, M. Power spectra of longitudinal and lateral wind speed near the ground in strong winds. *J. Wind Engng Indust. Aerodyn.*, Vol. 28, pp. 31-40, 1988.
47. HOXEY, R.P. Unpublished data, AFRC Engineering, Silsoe, Bedfordshire, England, 1990.

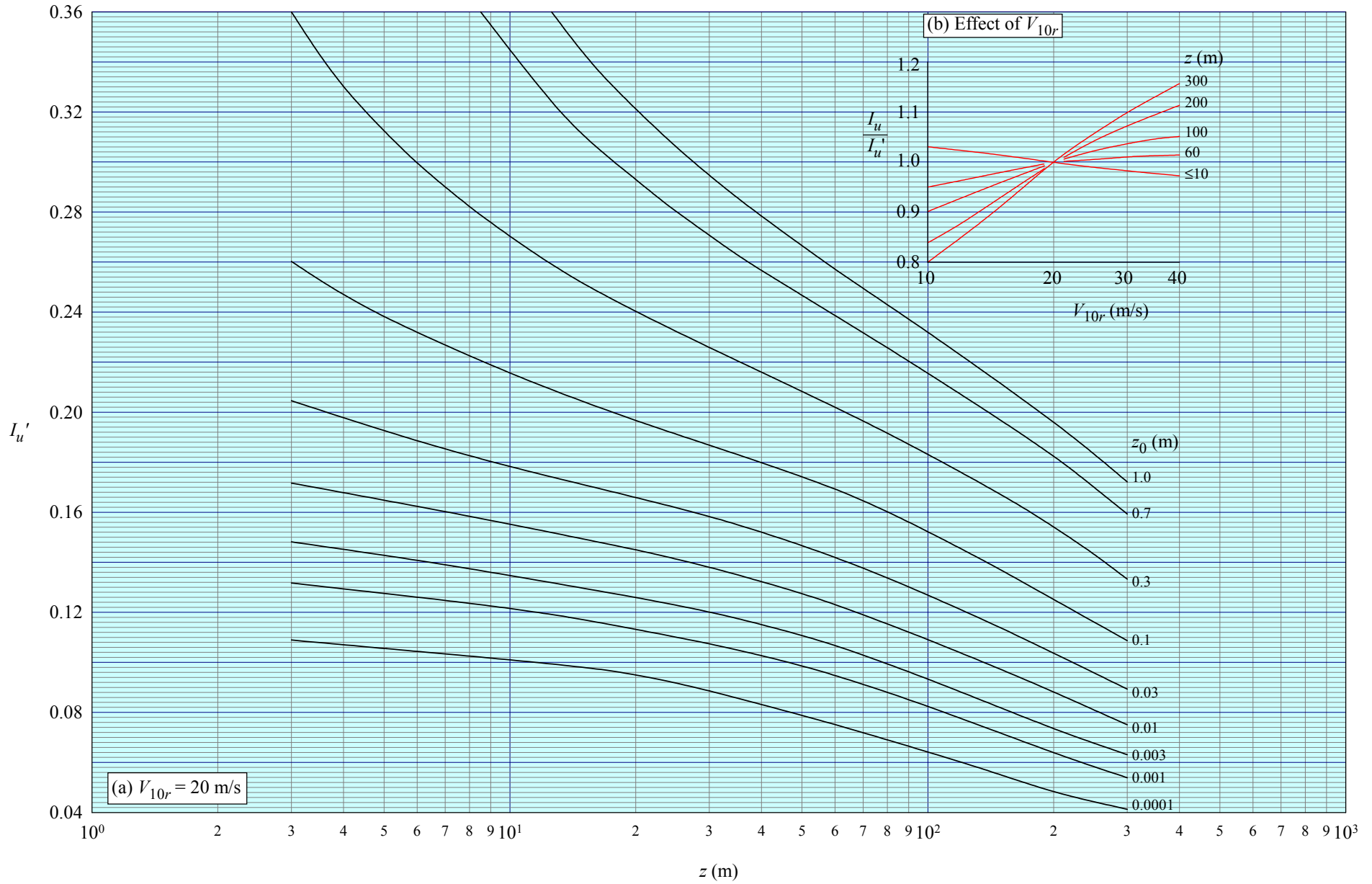


FIGURE 1 TURBULENCE INTENSITY FOR EQUILIBRIUM CONDITIONS

$$\sigma_v / \sigma_u = 1 - 0.22 \cos^4 \left(\frac{\pi}{2} \frac{z}{h} \right)$$

$$\sigma_w / \sigma_u = 1 - 0.45 \cos^4 \left(\frac{\pi}{2} \frac{z}{h} \right)$$

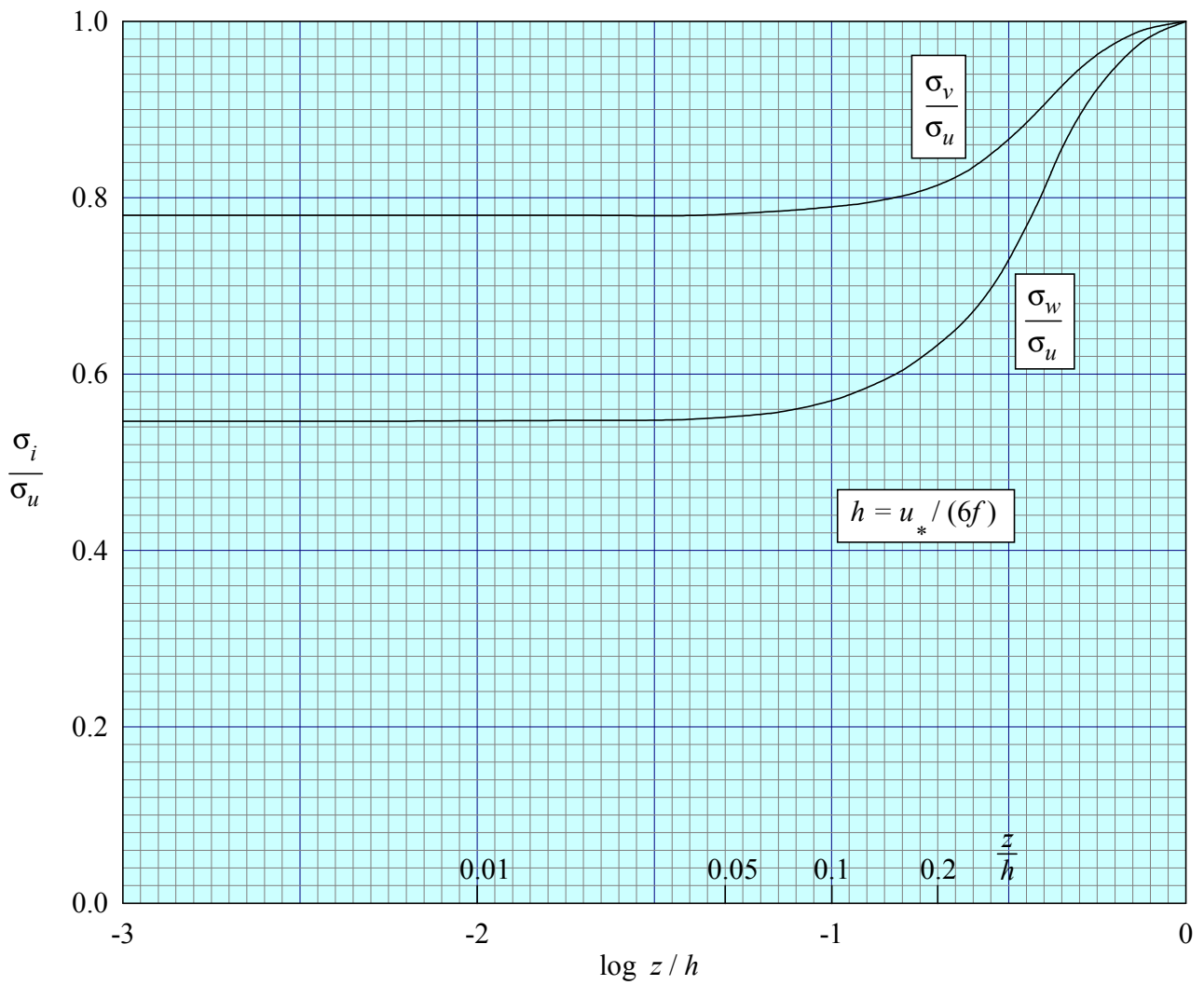


FIGURE 2 R.M.S. FLUCTUATING VELOCITIES OF v - AND w -COMPONENTS OF TURBULENCE

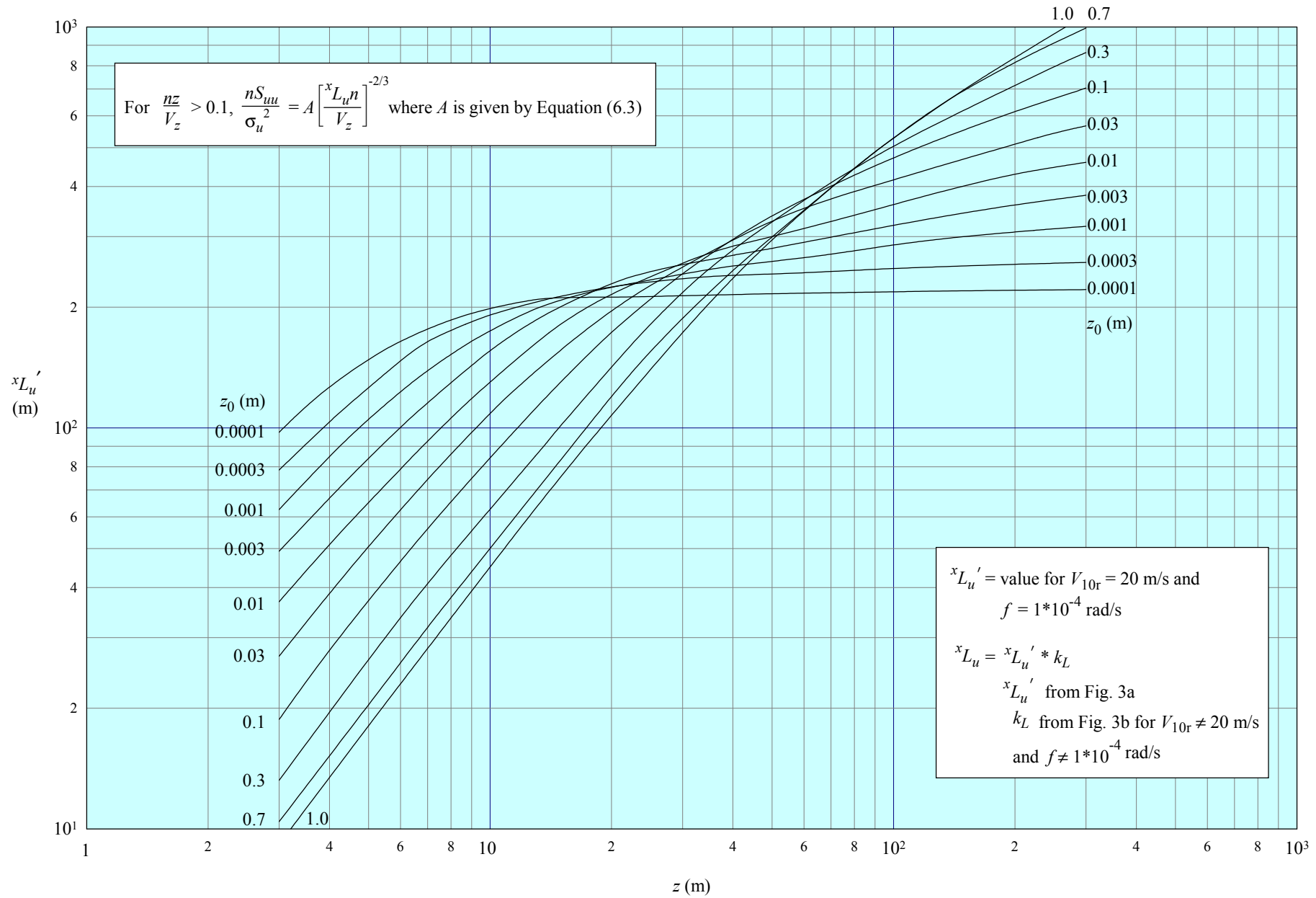


FIGURE 3a INTEGRAL LENGTH SCALE OF TURBULENCE FOR EQUILIBRIUM CONDITIONS. VALUES FOR $V_{10r} = 20 \text{ m/s}$ and $f = 1 \times 10^{-4} \text{ rad/s}$

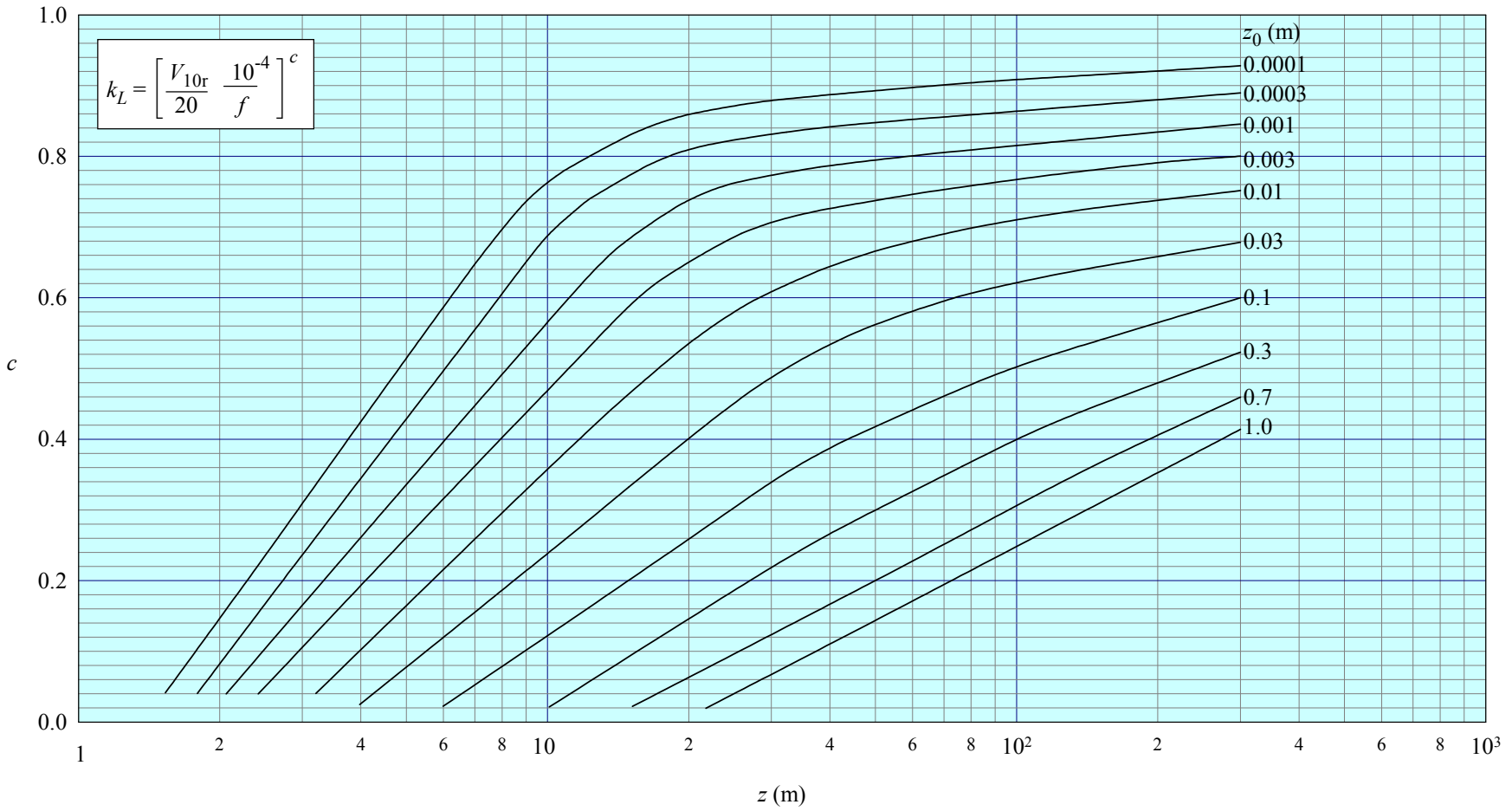


FIGURE 3b CORRECTION FACTOR FOR EFFECT OF V_{10r} AND f ON xL_u

APPENDIX A NOTES ON THE BASIS OF THE HIGH FREQUENCY SPECTRAL DATA AND LENGTH SCALES

A1. ADDITIONAL NOTATION

K_z	Kolmogorov parameter (Section A2.2)
K_0	value of K_z for $z \rightarrow 0$
n_i	$n^x L_i / V_z$ ($i = u, v$ or w)
Ro	surface Rossby number, $u_*/(fz_0)$
u_{*j}	value of u_* for fetch j where equilibrium conditions are assumed to exist upwind of j^{th} step change in roughness
u_{*0}	local value of u_* for $z \leq z_b$
z_b, z_u	internal boundary layer interface heights (see Sketch A3.1)

A2. DERIVATION OF SPECTRA AND LENGTH SCALES (EQUILIBRIUM BOUNDARY LAYER)

A2.1 Von Karman Model

The normally used forms of the von Karman spectral equations (as used in Item 74031 which this Item supersedes) are

$$\frac{nS_{uu}}{\sigma_u^2} = \frac{4n_u}{(1 + 70.8n_u^2)^{5/6}}; n_u = {}^xL_u n/V_z \quad (A2.1)$$

$$\frac{nS_{ii}}{\sigma_i^2} = \frac{4n_i(1 + 755.2n_i^2)}{(1 + 283.2n_i^2)^{11/6}}; n_i = {}^xL_i n/V_z; i = v \text{ or } w. \quad (A2.2)$$

In the high frequency region Equation (A2.1) reduces to

$$\frac{nS_{uu}}{\sigma_u^2} = 0.115 n_u^{-2/3} \quad (A2.3)$$

where $n_u = {}^xL_u n/V_z$ and xL_u is the longitudinal integral length scale of turbulence given by

$${}^xL_u = V_z \int_0^\infty \rho_{uu} d\tau. \quad (A2.4)$$

In Equation (A2.4), ρ_{uu} is the corresponding autocorrelation function (which is related to the spectral density function through the inverse Fourier transform). Where autocorrelations and spectra have both been

derived from field measurements it is found, consistently, that length scales (xL_u) derived using Equation (A2.4) are considerably greater than the length scales (xL_u)_s required in Equation (A2.3) to fit the measured spectral density data. This may be partly due to trends in the data but is mostly a result of the inadequacy of Equation (A2.1) (and the corresponding autocorrelation function) to represent the characteristics of turbulence closely at all frequencies (and time lags). To rectify this deficiency it is necessary to modify the form of Equation (A2.1) (see Appendix B) whilst still retaining the well established high frequency form

$$n S_{uu} / \sigma_u^2 = A ({}^xL_u n / V_z)^{-2/3}. \quad (\text{A2.5})$$

In order to satisfy the condition that the integral length scale, xL_u , given by Equation (A2.4) can be used in Equation (A2.5) the parameter A must be defined as

$$A = 0.115 [{}^xL_u / ({}^xL_u)_s]^{2/3}. \quad (\text{A2.6})$$

An analysis of good quality field data³⁵ for Rugby ($z_0 = 0.03$ m) and Cranfield ($z_0 = 0.003$ m), where as far as possible all significant trends are absent or have been removed, gives the approximate relationship that

$${}^xL_u / ({}^xL_u)_s = 1 + 0.315(1 - z/h)^6. \quad (\text{A2.7})$$

Equation (A2.7) is based on data for heights up to about 180 m.

A2.2 Kolmogorov Spectral Density Model

Harris and Deaves³⁹ show how the well established spectral density equation due to Kolmogorov, applicable to the high frequency region, can be used to derive an expression for spectral density which is dependent only on the mean wind speed profile parameters. The Kolmogorov equation is of the form

$$n S_{uu}(n) = K_z (\varepsilon V_z)^{2/3} n^{-2/3} \quad (\text{A2.8})$$

where ε is the energy dissipation given approximately by

$$\varepsilon \approx \frac{\tau_z}{\rho} \frac{dV_z}{dz} \quad (\text{A2.9})$$

and K_z is a Kolmogorov parameter for which laboratory measurements for isotropic turbulence have suggested a value of about 0.15 although measurements in the atmospheric boundary layer indicate higher values. In Equation (A2.9) Harris and Deaves represent the shear stress variation with height by

$$\frac{\tau_z}{\rho} = u_*^2 (1 - z/h)^2 \quad (\text{A2.10})$$

where ρ is the air density, h is the boundary layer (gradient) height ($= u_*/(6f)$) and

$$V_z = 2.5 u_* [\ln(z/z_0) + 5.75 z/h - 1.875(z/h)^2 - 1.333(z/h)^3 + 0.25(z/h)^4] \quad (\text{A2.11})$$

from which, for heights up to about 300 m,

$$\frac{dV_z}{dz} \approx 2.5u_*(1/z + 5.75/h). \quad (\text{A2.12})$$

Combining Equations (A2.8) to (A2.12) gives, for an equilibrium boundary layer under neutral stability conditions and ignoring small terms,

$$nS_{uu}(n) = 1.842K_z u_*^2 [(1 - z/h)^2 (1 + 5.75z/h)]^{2/3} [V_z/(nz)]^{2/3}. \quad (\text{A2.13})$$

Substituting for nS_{uu} , from Equation (A2.5), in Equation (A2.13) it follows that, for heights up to about 300 m, xL_u can be expressed as

$$^xL_u = \frac{A^{3/2}(\sigma_u/u_*)^3 z}{2.5K_z^{3/2}(1 - z/h)^2 (1 + 5.75z/h)} \quad (\text{A2.14})$$

with A (from Equations (A2.6) and (A2.7)) given by

$$A = 0.115[1 + 0.315(1 - z/h)^6]^{2/3}. \quad (\text{A2.15})$$

It should be emphasised that, for the reasons discussed in Section A2.1, length scales obtained through Equation (A2.14) are derived for compatibility with the spectral density function given by Equation (A2.5) with A given by Equations (A2.6) and (A2.7). By comparison, length scales derived for use with the von Karman form of spectral density equation will be *smaller* by a factor given by the reciprocal of Equation (A2.7); for heights near the ground (less than about 30 m) this factor is about 0.7.

Harris and Deaves³⁹ found that in fitting Equation (A2.13) to good quality field measurements for Rugby and Cranfield it was necessary to allow K_z to vary with height. A best fit of Equation (A2.13) to the data gave

$$K_z = K_\infty[1 - (1 - z/z_c)^2]^{1/2} \text{ or } K_z = K_\infty \text{ for } z > z_c \quad (\text{A2.16})$$

where $z_c/h = 0.39[u_*/(fz_0)]^{-1/8}, \quad (\text{A2.17})$

with $h = u_*/(6f)$ and $K_\infty = 0.188$.

However, it has been recognised that close to the ground further development of this model is required for the following reasons.

As noted in Section 7.1, consideration of similarity theory leads to the result that length scales of turbulence should be scaled in relation to boundary layer depth, h , (that is, eddies are stretched in size with increasing h). With increasing wind speed and terrain roughness, h increases so that in accordance with similarity theory length scales (at a given height) will increase accordingly. However, in a region close to the ground, wind speed and turbulence properties are more closely related to z/z_0 so that length scales (at a given height) should be smaller for rougher terrain, and there will be little or no dependence on wind speed. Equation (A2.14) with K_z given by Equation (A2.16) provides values of xL_u in accordance with the first similarity requirement but, as was recognised at the time, it did not exhibit an independence of wind speed close to the ground; a lack of reliable measured data in this region prevented further development of the model.

A re-analysis of the data^{A1}, incorporating more recent data obtained from measurements relatively close to the ground, suggests that the variation of the Kolmogorov parameter, K_z , with height follows the general trend given by Equation (A2.16) but with the difference that it tends to an asymptotic value (K_0) at low heights and, additionally, is dependent on terrain roughness (or more specifically the non-dimensional surface Rossby number, $Ro = u_*/(fz_0)$). The empirical relationship derived for K_z is illustrated in Sketch A2.1 and is given by

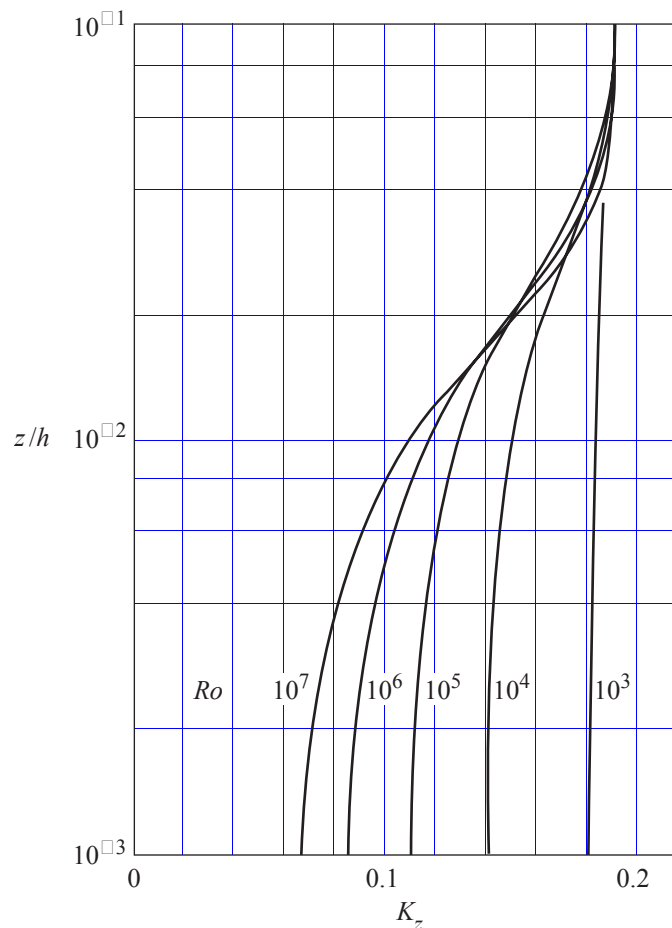
$$K_z = 0.19 - (0.19 - K_0) \exp[-B(z/h)^N] \quad (\text{A2.18})$$

where
$$K_0 = \frac{0.39}{Ro^{0.11}}, \quad (\text{A2.19})$$

$$B = 24Ro^{0.155}, \quad (\text{A2.20})$$

$$N = 1.24Ro^{0.008} \quad (\text{A2.21})$$

and
$$Ro = \frac{u_*}{fz_0}.$$



Sketch A2.1

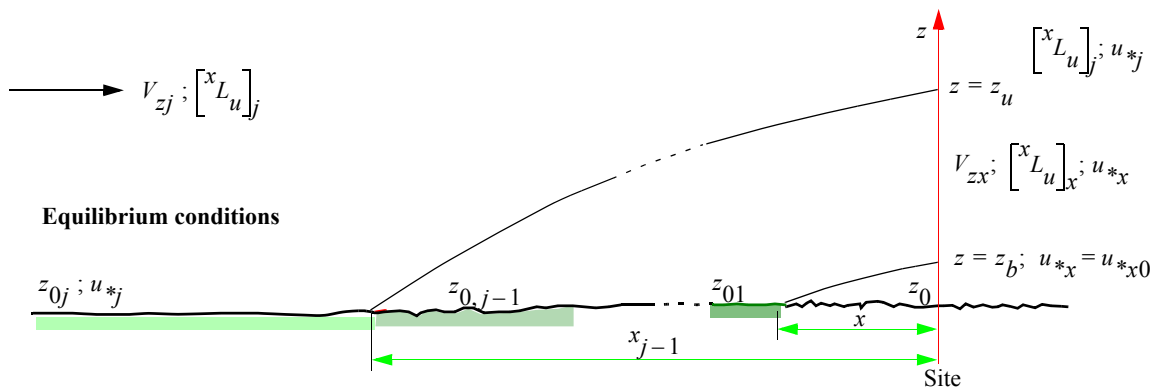
A close approximation to values of xL_u given by Equation (A2.14) using values of K_z from Equation (A2.18) is presented in Figure 3 and is similar in value to that previously obtained at comparatively large heights above the ground ($z/h > 0.1$). However, closer to the ground the present values of xL_u (Figure 3) are essentially independent of wind speed and decrease in value as z_0 increases.

The bulk of the spectral data used in the analysis^{A1} for K_z were for sites with essentially uniform terrain which is usually open country. However, some data were obtained from off-shore installations where z_0 is significantly smaller and for which the effect of terrain roughness on K_z close to the ground is more apparent.

Other data used originate from sites where changes occur in the terrain roughness upwind of, and relatively close to, the site such as in the case of built-up areas. In these cases it is necessary to use local values of the parameters such as u_{*x} , V_{zx} and h_x (as described in Section A3) to back-calculate values of K_z using Equation (A2.13). This was achieved using the computer program described in Item 92032¹⁰.

A3. NON-EQUILIBRIUM BOUNDARY LAYER

No definitive method exists for predicting spectral density within a non-equilibrium boundary layer. For a single roughness change an estimate may be made for the high frequency range through Equation (A2.13) by using local values of the parameters involved.



Sketch A3.1

In the region above $z = z_u$ (see Sketch A3.1) the properties of turbulence (and wind speed) are largely unaffected by the roughness changes and in this region values of spectral density are given by Equation (A2.13) with $u_* = u_{*j}$, $z_0 = z_{0j}$ and $V_z = V_{zj}$.

In the lowest layer near the ground (strictly $z < z_b$) Equation (A2.13) applies providing u_* is replaced by u_{*x} . It then follows, to close approximation, that for each height $z < z_b$

$$[^xL_u]_x / ^xL_u \approx (I_{ux} / I_u)^3 \quad (\text{A3.1})$$

where xL_u and I_u are the length scale and turbulence intensity at the site under equilibrium conditions (ideally when $x > 600$ km) and I_{ux} ($= \sigma_{ux} / V_{zx}$) is the local turbulence intensity taking into account the upwind roughness change.

In the transition zone $z_b < z < z_u$ the effective friction velocity, u_{*x} , varies between $u_{*x} = u_{*x0}$ for $z < z_b$ and u_{*j} for $z > z_u$; the effective z_{0x} also varies between z_0 and z_{0j} . For a single roughness change ($j = 1$) Deaves provides empirical fits to theoretically derived mean-wind (V_{zx}) and turbulence (σ_{ux}) profiles from which it is possible to derive analytical expressions for the variations of u_{*x} , z_{0x} and dV_{zx}/dz with height. When these expressions are used in Equations (A2.8) to (A2.12) equivalent values of $[n S_{uu}]_x$ are obtained. Similarly, Equation (A2.5) provides values of $[n S_{uu}]_x$ by substituting local values of V_{zx} and σ_{ux}^2 . By equating values of $[n S_{uu}]_x$ from the two methods it is then possible to evaluate the variation of $[^xL_u]_x$ for different combinations of step changes in terrain roughness (z_{01} to z_0) and fetch, x , as described in Section A3.1.

It then follows that the local spectral density is given by Equation (A2.5) with $[^xL_u]_x$, V_{zx} and σ_{ux} substituted for xL_u , V_z and σ_u . Values of I_{ux} ($= \sigma_{ux}/V_{zx}$), V_{zx} and $[^xL_u]_x$ can be obtained from the tables in Items 84030⁸, 84011⁷ and 86035⁹ respectively for typical site terrains. Alternatively, the computer program given in Item 92032¹⁰ can be used for multiple roughness changes.

A3.1 Equations for Calculating Local Values of $[^xL_u]_x$ for Single Roughness Change

The equations given by Deaves^{41, 42} for the variation of u_{*x} , z_{0x} and σ_{ux} , relating to a single roughness change, are summarised by Equations (A3.4) to (A3.7) and Table A3.1. Additionally, the wind shear, dV_{zx}/dz , is required to evaluate $[^xL_u]_x$. This can be obtained by differentiating the equations for the mean wind speed profile given by Deaves which take the same form as for an equilibrium boundary layer but with values of u_{*x} and z_{0x} which vary with z . A simplified equation for dV_{zx}/dz has been adopted. This form is derived by differentiating Equation (A2.11) (which is applicable throughout the atmospheric boundary layer under equilibrium conditions) with the result that

$$\frac{1}{u_*} \frac{dV_z}{dz} = (2.5/z)(1 + 5.75z_1 - 3.75z_1^2 - 4z_1^3 + z_1^4) \quad (\text{A3.2})$$

where $z_1 = z/h$. In theory, dV_{zx}/dz is also dependent on terms involving du_{*x}/dz and dz_{0x}/dz but since these terms are of opposite sign a good approximation to dV_{zx}/dz is obtained through Equation (A3.2) but replacing u_* and h by their local values (u_{*x}) and $h_x = u_{*x}/(6f)$.

Clearly, the combination of all the equations given below is not ideally suited to hand calculations. For convenience these equations have been programmed and tables of length scales computed for a range of heights and combinations of terrain roughness at, and upwind of, the site. These tables are presented in Item 86035⁹. Alternatively, the computer program given in Item 92032¹⁰ can be used for more complex situations.

The local length scale $[^xL_u]_x$ is given by

$$[^xL_u]_x = \frac{A^{3/2} \sigma_{ux}^3}{K_z^{3/2} \epsilon} = \frac{A^{3/2} (\sigma_{ux}/u_{*x})^3}{K_z^{3/2} (1 - z/h_x)^2 (dV_{zx}/dz)/u_{*x}} \quad (\text{A3.3})$$

The parameters A and K_z are given by Equations (A2.15) and (A2.18) using local site values of h_x and u_{*x} ; the parameters σ_{ux} , u_{*x} , $h_x = u_{*x}/(6f)$ and dV_{zx}/dz depend on whether $z_{01} < z_0$ or $z_{01} > z_0$.

In general, for $z_{01} > z_0$ or $z_{01} < z_0$.

$$u_{*x} = (u_{*x0} - u_{*1}) \cos^2(\theta_2/2) + u_{*1} \quad (\text{A3.4})$$

$$u_{*x0} = (K_{x2} u_{*1}) \quad (\text{see Table A3.1}) \quad (\text{A3.5})$$

$$\ln z_{0x} = \ln(z_0/z_{01}) \cos^2(\theta_1/2) + \ln z_{01} \quad (\text{A3.6})$$

$$\sigma_{ux} = \sigma_u - (\sigma_u - \sigma_{u1}) \cos^2 \theta_3 \quad (\text{A3.7})$$

and $(dV_{zx}/dz)/u_{*x}$ is given by Equation (A3.2) with $u_* = u_{*x}$ and $h = u_{*x}/(6f)$.

Table A3.1 tabulates expressions for the various parameters in Equations (A3.4) to (A3.7) relating to a single roughness change.

In Table A3.1 the factor K_{x2} which equals u_{*x0}/u_{*1} (the ratio of the actual friction velocity close to the surface at the site to the upwind equilibrium value) is taken from Item 92032. It is derived from equations given by Harris and Deaves³⁹ but corrected through the factor K_u to account for deficiencies in the theory as the fetch, x , tends to F (the fetch required for equilibrium conditions to exist over the site).

The equations from which the parameters u_{*x} , z_{0x} and dV_{zx}/dz are derived were obtained by Deaves by fitting suitable expressions to theoretically derived data. As a result, when they are used in the way described to derive $[^xL_u]_x$ through Equation (A3.3), small inconsistencies occur which are reflected in some non-uniform variations with z and x of computed values of $[^xL_u]_x$. No attempt has been made to 'smooth' these variations. Non-uniform variations of length scale with changing x and z must be expected in some cases since, unlike σ_u and V_z , length scales tend to an asymptotic value at large heights which depends on the boundary-layer height, h (which varies with z_0 for a given V_{10r}).

TABLE A3.1 Expressions for Parameters in Equations (A3.4) to (A3.7) for Single ($j = 1$) Step Change in Terrain Roughness Upwind of Site

	$z_{01} \leq z_0$	$z_{01} \geq z_0$
z_b	$0.00406 z_0^{0.0476} x^{0.952}$	$0.7 x^{0.6} (z_0^{0.6}/z_{01}^{0.68})$
z_i	$0.36 x^{3/4} z_0^{1/4}$	$0.7 x (z_0/z_{01})^{1/2}$
z_t	$10 x^{0.6} z_0^{0.4}$	$10 x^{0.6} z_{01}^{0.4}$
z_u	$14.2 x^{0.6} z_0^{0.4}$	$10 x^{0.6} z_{01}^{0.4}$
ζ	$\ln(z/z_t)$	$\ln(z/z_i)/\ln(z_t/z_i)$
θ_1	$(\pi/4)(\zeta + 3.2)$ $\theta_1 = 0$ for $\zeta \leq -3.2$; $\theta_1 = \pi$ for $\zeta \geq 0.8$	$(\pi/1.2)(\zeta + 0.2)$ $\theta_1 = 0$ for $\zeta \leq -0.2$; $\theta_1 = \pi$ for $\zeta \geq 1.0$
θ_2	$(\pi/4)(\zeta + 3.65)$ $\theta_2 = 0$ for $\zeta \leq -3.65$; $\theta_2 = \pi$ for $\zeta \geq 0.35$	$= \theta_1$ for $z_{01} \geq z_0$
x_i	$(z/0.36)^{4/3}/z_0^{1/3}$	$(z/0.07)(z_{01}/z_0)^{1/2}$
x_t	$(0.1z)^{5/3}/z_0^{2/3}$	$(0.1z)^{5/3}/z_{01}^{2/3}$
ξ	$\ln(x/x_t)/\ln(x_i/x_t)$	$\ln(x/x_t)/\ln(x_i/x_t)$
θ_3	$(\pi/4)(\xi - 0.25)/0.8$ $\theta_3 = 0$ for $\xi \leq 0.25$; $\theta_3 = \pi/2$ for $\xi \geq 1.85$	$(\pi/4)(\xi - 0.1)/0.8$ $\theta_3 = 0$ for $\xi \leq 0.1$; $\theta_3 = \pi/2$ for $\xi \geq 1.7$
K_{x2}	$\frac{u_{*x0}}{u_{*1}} = 1 - \frac{K_u \ln(z_{01}/z_0)}{0.0106 x_2^2 + 0.61 x_2 + 0.316}$ $K_u = 1 - k_1(1 - K_{uf})$ $k_1 = 0.29 \ln(xF) + 1$: if $k_1 < 0$ then $k_1 = 0$; if $k_1 > 1.0$ then $k_1 = 1.0$ $K_{uf} = 0.54 + 0.019 \ln(F/z_0)$ $F =$ values of x for equilibrium conditions to be established	with $x_2 = \ln(x/z_0)$
	For $z_{01} < z_0$ $F = 0.358 (u_{*}/f)^{4/3} (1/z_0)^{1/3}$	For $z_{01} > z_0$ $F = 2.33 (u_{*}/f)(z_{01}/z_0)^{1/2}$

A3.2 Multiple Roughness Changes

The equations in Section A3.1 are strictly valid only for a single roughness change upwind of the site. They can be used to generate data for more than one roughness change using the following procedure which approximates the problem to a series of single roughness changes.

For the roughness change z_{0j} to z_{0j-1} (see Sketch A3.1) use the equations provided (with $z_{0j}=z_{01}$, $z_{0j-1}=z_0$ etc.) to calculate local values of the parameters $(u_{*x})_{j-1}$, $(u_{*x0})_{j-1}$ and $(\sigma_{ux})_{j-1}$ at height z over the location of the site. These values are then used as input data ($(u_{*x})_{j-1}=u_{*1}$, etc.) for the next downwind roughness change and the process repeated until all roughness change effects upwind of the site (that will affect conditions at height z) have been accounted for. The local values of u_{*x} , σ_{ux} , etc. are then used in Equation (A3.5) to determine $[^xL_u]_x$. This procedure is the basis of the method programmed in Item 92032¹⁰.

A3.3 Comparison With Measured Data

There are few reliable data against which the methods accounting for roughness changes can be checked. Some reported spectral measurements (for example, Derivations 13, 18, 30, 32, 43, 46, 47) taken at sites with changes in the upwind terrain roughness have been used to compare turbulence properties derived from the measured data with corresponding predicted values. At heights near the ground ($z < 30$ m) the measured values can be reproduced to within about $\pm 15\%$ in I_{ux} and about $\pm 30\%$ in spectral density for the better quality records. However, there can be considerable variations in the measured quantities derived from individual runs. At larger heights, due to uncertainties in wind direction and type of terrain further upwind, quantitative comparisons between measured and predicted values are less reliable, particularly where multiple roughness changes are involved, although qualitatively the correct trends can be reproduced when the existence of upwind changes in terrain roughness are taken into account rather than ignored.

A4. ADDITIONAL REFERENCES

- A1. THOMPSON, N. Integral length scales of turbulence: a re-analysis including data for non-uniform terrain. ESDU Memorandum No. 76, 1990.

APPENDIX B MODIFIED VON KARMAN SPECTRAL EQUATIONS (AND AUTOCORRELATION FUNCTIONS) FOR COMPLETE FREQUENCY RANGE

B1. ADDITIONAL NOTATION

A	constant in spectral density equation for high frequency range, see Equation (B5.6)
F_1, F_2	functions of n_i/α used in Equations (B4.1), (B4.2) and given by Equations (B4.3), (B4.4)
f	longitudinal autocorrelation function, $\rho_{uu}\{\tau\}$, equivalent to $\rho_{uu}\{\Delta x\}$, or $\rho_{vv}\{\Delta y\}$ or $\rho_{ww}\{\Delta z\}$ for $\tau = 0$
g	lateral autocorrelation function, $\rho_{vv}\{\tau\}$, or $\rho_{ww}\{\tau\}$, equivalent to $\rho_{uu}\{\Delta y \text{ or } \Delta z\}$, or $\rho_{vv}\{\Delta x \text{ or } \Delta z\}$ or $\rho_{ww}\{\Delta x \text{ or } \Delta y\}$ for $\tau = 0$
$K_v\{X\}$	modified Bessel function of second kind of order v and argument X
M_v	$X^v K_v\{X\}$
\tilde{r}_f	longitudinal non-dimensional separation; $\Delta x/x L_u, \Delta y/y L_v, \Delta z/z L_w$
\tilde{r}_g	lateral non-dimensional separation; $\Delta x/(2^x L_i)$ for $i = v, w$; $\Delta y/(2^y L_i)$ for $i = u, w$; $\Delta z/(2^z L_i)$ for $i = u, v$
T	integral time scale of turbulence
α, β	factors in modified von Karman equations (see Section B5)
τ	incremental time lag
ξ	function of $\alpha\tau/T$, see Equation (B3.2)

B2. BACKGROUND

The von Karman equations have been recognised for many years as the best available description of turbulence spectra for strong winds. However, there is evidence that this model has some deficiencies; these are as follows.

- (i) Below about 100 m the integral length scales as derived using an integration of measured autocorrelation functions tend to be larger than those obtained by fitting the von Karman spectral equation to measured data in the high frequency region. This is discussed more fully in Section A2.1 of Appendix A where a high frequency form of the von Karman spectral equations is derived to take this deficiency into account. In the high frequency limit the model discussed in this Appendix reverts to that given in Appendix A.
- (ii) Where the quality of measured data has been adequate to determine the true peak value of nS_{uu}/σ_u^2 (and also nS_{vv}/σ_v^2 and nS_{ww}/σ_w^2) in measured spectra it is found that this peak value tends to be smaller than that given by the von Karman equations at heights near the ground.

Above about 150 m the von Karman spectral equations appear to represent measured data reasonably well

providing the length scale appropriate to the terrain and height over the site is used. In order to alleviate the deficiencies at lower heights a modified von Karman model has been derived. The full details of the derivation are given by Harris^{B1} but the following points, which provide constraints on a new formulation, are worth summarising here.

Spectral density and autocorrelation functions are Fourier transforms of each other so that (for $i = u, v$ or w)

$$\rho_{ii} = \frac{1}{\sigma_i^2} \int_0^\infty S_{ii} \cos(2\pi n\tau) \, dn \quad (\text{B2.1})$$

$$S_{ii} = 4\sigma_i^2 \int_0^\infty \rho_{ii} \cos(2\pi n\tau) \, d\tau \quad (\text{B2.2})$$

from which for $\tau = 0$ and $n = 0$

$$\int_0^\infty S_{ii}/\sigma_i^2 \, dn = 1 \quad (\text{B2.3})$$

$$S_{ii}(n = 0) = 4\sigma_i^2 \int_0^\infty \rho_{ii} \, d\tau = 4\sigma_i^2 T \quad (\text{B2.4})$$

where $T = {}^rL_i/V_z$. Furthermore, for large values of nT (see Section A2 of Appendix A)

$$nS_{ii}/\sigma_i^2 \approx A(nT)^{-2/3} \quad (\text{B2.5})$$

The von Karman equations satisfy all these constraints and any modification to them must also comply.

B3. MODIFIED EQUATIONS FOR AUTOCORRELATION FUNCTIONS

Several possible modifications to the von Karman equations have been investigated^{B1} but the most viable one involves using an autocorrelation function represented by a functional series of the form

$$\rho_{uu} = \beta_1 \xi + \beta_2 \xi^2 + \beta_3 \xi^3 + \dots \quad (\text{B3.1})$$

where the function ξ has the von Karman form

$$\xi = 0.593(\alpha\tau/T)^{1/3} K_{1/3}\{\alpha\tau/T\} \quad (\text{B3.2})$$

$$= 0.593(\alpha\tilde{r}_f)^{1/3} K_{1/3}(\alpha\tilde{r}_f) \quad (\text{B3.3})$$

and $\tilde{r}_f = \tau/T = \tau V_z / {}^xL_u = \Delta x / {}^xL_u$ by Taylor's hypothesis of frozen turbulence being advected along wind at a speed of V_z . The factor α is determined in order to satisfy Equation (A2.4) and is dependent on the values β_1, β_2 etc. and A (see Section B5). Note that when $\beta_1 = 1$ and $0 = \beta_2 = \beta_3$ etc. then the von Karman form of autocorrelation is obtained with $\alpha = \pi^{1/2} \Gamma_{5/6} / \Gamma_{1/3} = 0.747$.

In order to avoid over-complexity, the functional series (Equation (B3.1)) is limited to two terms with β_1

and β_2 only. The longitudinal autocorrelation function ($\rho_{uu}\{\tau\}=f$) then becomes

$$f = \beta_1 \xi + \beta_2 \xi^2 \quad (\text{B3.4})$$

where ξ is given by Equation (B3.3).

The lateral autocorrelation function, g , for the $i = v$ - and w -components can be obtained from f using the condition for flow continuity which for isotropic turbulence is

$$g = f + \frac{1}{2} \Delta r \frac{df}{d(\Delta r)} \quad (\text{B3.5})$$

where Δr is equated to τV_z . Reference B1 shows that this results in

$$g = 0.593 \beta_1 \left[M_{1/3} - \frac{1}{2} (\alpha \tilde{r}_g)^{2/3} M_{2/3} \right] + 0.351 \beta_2 [M_{1/3} - (\alpha \tilde{r}_g)^{2/3} M_{1/3} M_{2/3}] \quad (\text{B3.6})$$

where, for notational convenience, $M_v = (\alpha \tilde{r}_g)^v K_v\{\alpha \tilde{r}_g\}$ and $\tilde{r}_g = \tau/T$ which is equated to $\tilde{r}_g = \Delta x / (2^x L_i)^*$.

Equations (B3.4) and (B3.6) for f and g with appropriate values of the factors α , β_1 and β_2 taken from Section B5 are plotted in Figure B1. Simplified equations for these functions are given in Section B3.1.

B3.1 Simplified Equations for the Autocorrelation Functions

To avoid the need to evaluate the Bessel functions in Equations (B3.4) and (B3.6) the functions f and g are plotted in Figure B1 as a function of \tilde{r}_f (or \tilde{r}_g) and z/h . It is clear that the effect of z/h on ρ_{ii} is small and for simplicity good approximations that closely represent the true variation of f with \tilde{r}_f and g with \tilde{r}_g are given by the following equations[†]

$$\rho_{uu} = f = \frac{1}{2} (f_1 + f_1^2) \quad (\text{B3.7})$$

where $f_1 = \exp(-0.822 \tilde{r}_f^{0.77}) \quad (\text{B3.8})$

with $\tilde{r}_f = \tau V_z / {}^x L_u = \Delta x / {}^x L_u$. (B3.9)

For the $i = v$ - or w -component

$$\rho_{ii} = g = \frac{1}{2} (g_1 + g_1^2) \quad (\text{B3.10})$$

where $g_1 = \exp(-1.23 \tilde{r}_g^{0.85}) \quad (\text{B3.11})$

with $\tilde{r}_g = \tau V_z / (2^x L_i)$. (B3.12)

* The factor '2' appears in the definition of \tilde{r}_g arising from the conditions for flow continuity (Equation B3.5). This gives the result that, for $i = v$ or w , ${}^x L_i = \int g d(\Delta r) = \frac{1}{2} \int f d(\Delta r) = \frac{1}{2} {}^x L_u$ for isotropic turbulence.

† Note that the approximate equations are not used in the Fourier transform process to obtain the corresponding spectral equations given in Section B4.

B4. MODIFIED EQUATIONS FOR SPECTRAL DENSITY FUNCTIONS

The corresponding equations for spectral density are obtained from the Fourier transform of the f and g functions for the u and for the $i = v$ - or w -component respectively. These are derived in Reference B1 and are as follows.

For the u -component

$$\frac{nS_{uu}}{\sigma_u^2} = \beta_1 \frac{2.987 n_u / \alpha}{[1 + (2\pi n_u / \alpha)^2]^{5/6}} + \beta_2 \frac{1.294 n_u / \alpha}{[1 + (\pi n_u / \alpha)^2]^{5/6}} F_1 \quad (\text{B4.1})$$

where $n_u = n^x L_u / V_z$.

For the $i = v$ - or w -component

$$\frac{nS_{ii}}{\sigma_i^2} = \beta_1 \frac{2.987 [1 + (8/3)(4\pi n_i / \alpha)^2] (n_i / \alpha)}{[1 + (4\pi n_i / \alpha)^2]^{11/6}} + \beta_2 \frac{1.294 n_i / \alpha}{[1 + (2\pi n_i / \alpha)^2]^{5/6}} F_2 \quad (\text{B4.2})$$

where $n_i = n^x L_i / V_z$.

The factors F_1 and F_2 in Equations (B4.1) and (B4.2) are functions of n_i / α and involve particular orders of the Gauss Hypergeometric Function which, although relatively simple to evaluate as a series expansion, are not familiar to most engineers. Details of these functions are given in Reference B1 but for the purpose of evaluating Equations (B4.1) and (B4.2) the factors F_1 and F_2 can be closely approximated by

$$F_1 = 1 + 0.455 \exp \left[-0.76 n_u / \alpha^{-0.8} \right], \quad (\text{B4.3})$$

$$F_2 = 1 + 2.88 \exp \left[-0.218 n_i / \alpha^{-0.9} \right]. \quad (\text{B4.4})$$

Equations (B4.1) and (B4.2) with appropriate values of the factors α , β_1 and β_2 from Section B5 are plotted in Figures B2 and B3 which show that the peak value of nS_{ii}/σ_i^2 decreases with height which tends to correct the deficiency noted in (ii) of Section B2.

The first term in each of Equations (B4.1) and (B4.2), with $\beta_1 = 1$ and $\alpha = 0.747$, gives the original von Karman spectral density equations for the u and $i = v$ - or w -component noted in Section A2.1 of Appendix A. Furthermore, at high frequencies, Equation (B4.1) reduces to the simple form

$$\frac{nS_{uu}}{\sigma_u^2} = A n_u^{-2/3} \quad (\text{B4.5})$$

compatible with Equation (6.2); similarly the v - and w -spectra reduce to a form compatible with Equation (6.4)

B5. EXPRESSIONS FOR α , β_1 AND β_2

At high frequencies, Equation (B4.1) reduces to

$$nS_{uu}/\sigma_u^2 = 0.1396 (\beta_1 + 2\beta_2)(n_u/\alpha)^{-2/3} \quad (\text{B5.1})$$

which equates to Equation (A2.5) in Appendix A so that

$$A/\alpha^{2/3} = 0.1396 (\beta_1 + 2\beta_2). \quad (\text{B5.2})$$

To satisfy the integral constraint of Equation (B2.4), α must be given by

$$\alpha = 0.747\beta_1 + 0.323\beta_2 \quad (\text{B5.3})$$

and to satisfy the condition that $\rho(\tau = 0) = 1.0$

$$\beta_1 + \beta_2 = 1.0. \quad (\text{B5.4})$$

For the original von Karman equation the factor $A = 0.115$. Departure from this value is desirable at heights near the ground in order to account for the observed deficiency that the ratio of the length scale derived from the autocorrelation function to that obtained from the spectral density function (at high frequencies) tends to be greater than unity. This ratio (l_s) as obtained from measured data exhibits wide scatter but the general trend of those observations considered to be most reliable (*i.e.* those without trends in the data) is represented by

$$l_s = 1 + 0.315 (1 - z/h)^6 \quad (\text{B5.5})$$

so that, by Equation (A2.6),

$$A = 0.115 [1 + 0.315(1 - z/h)^6]^{2/3}. \quad (\text{B5.6})$$

As $z/h \rightarrow 1.0$, $A \rightarrow 0.115$, $\beta_1 \rightarrow 1.0$, $\beta_2 \rightarrow 0$ and $\alpha \rightarrow 0.747$, *i.e.* the von Karman equation values. When $z/h = 0$, the maximum value of $A = 0.42$ is obtained, with $\beta_1 = \beta_2 = 0.5$ and $\alpha = 0.535$. To obtain even higher values of A further terms in the series represented by Equation (B3.1) would need to be considered.

From Equations (B5.2) to (B5.4) it follows that

$$\beta_2 = 1 - \beta_1, \quad (\text{B5.7})$$

$$\beta_1 = 2.357\alpha - 0.761, \quad (\text{B5.8})$$

$$\text{and} \quad A = \alpha^{2/3} (0.3858 - 0.3298\alpha). \quad (\text{B5.9})$$

Equation (B5.9) is a non-linear equation in α and a close approximation is given by

$$\alpha = 0.535 + 2.76(0.138 - A)^{0.68} \quad (\text{B5.10})$$

with A given by Equation (B5.6).

B6. ADDITIONAL REFERENCE

- B1. HARRIS, R. I. Some further thoughts on the spectrum of gustiness in strong winds.
J. Wind Engng Indust. Aerodyn., Vol. 33, pp. 461-477, 1990.

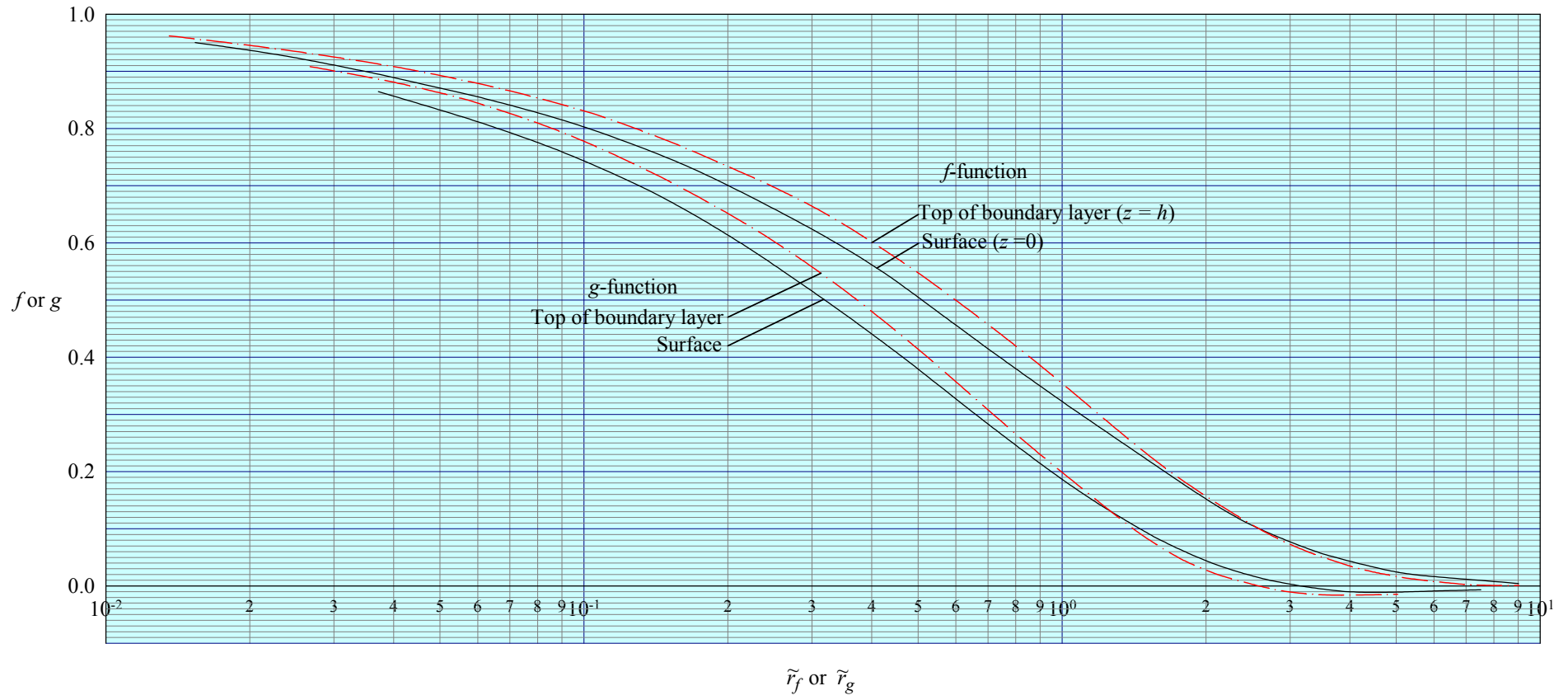


FIGURE B1 AUTOCORRELATION FUNCTIONS f AND g

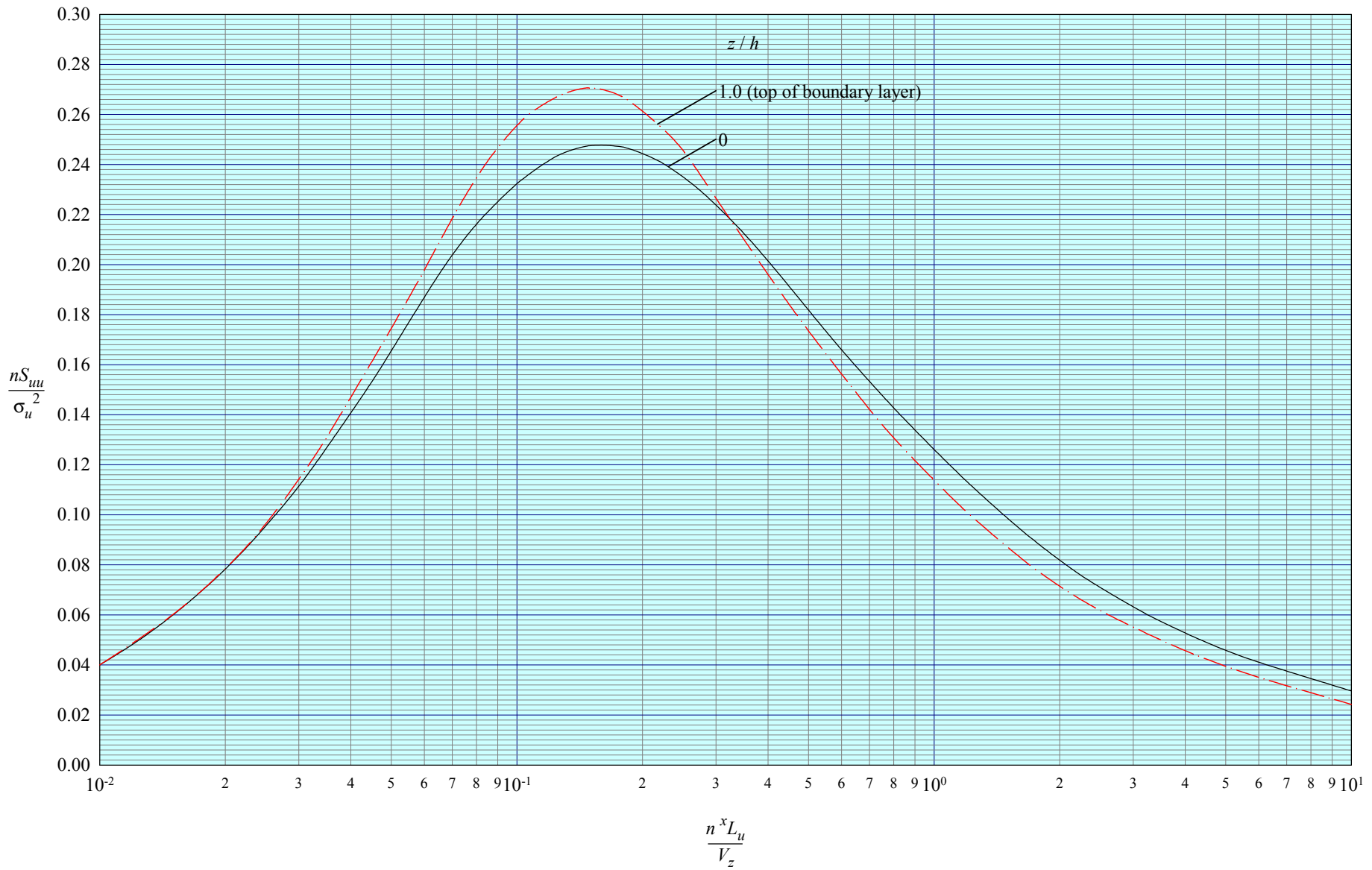


FIGURE B2 SPECTRAL DENSITY FUNCTION FOR u -COMPONENT

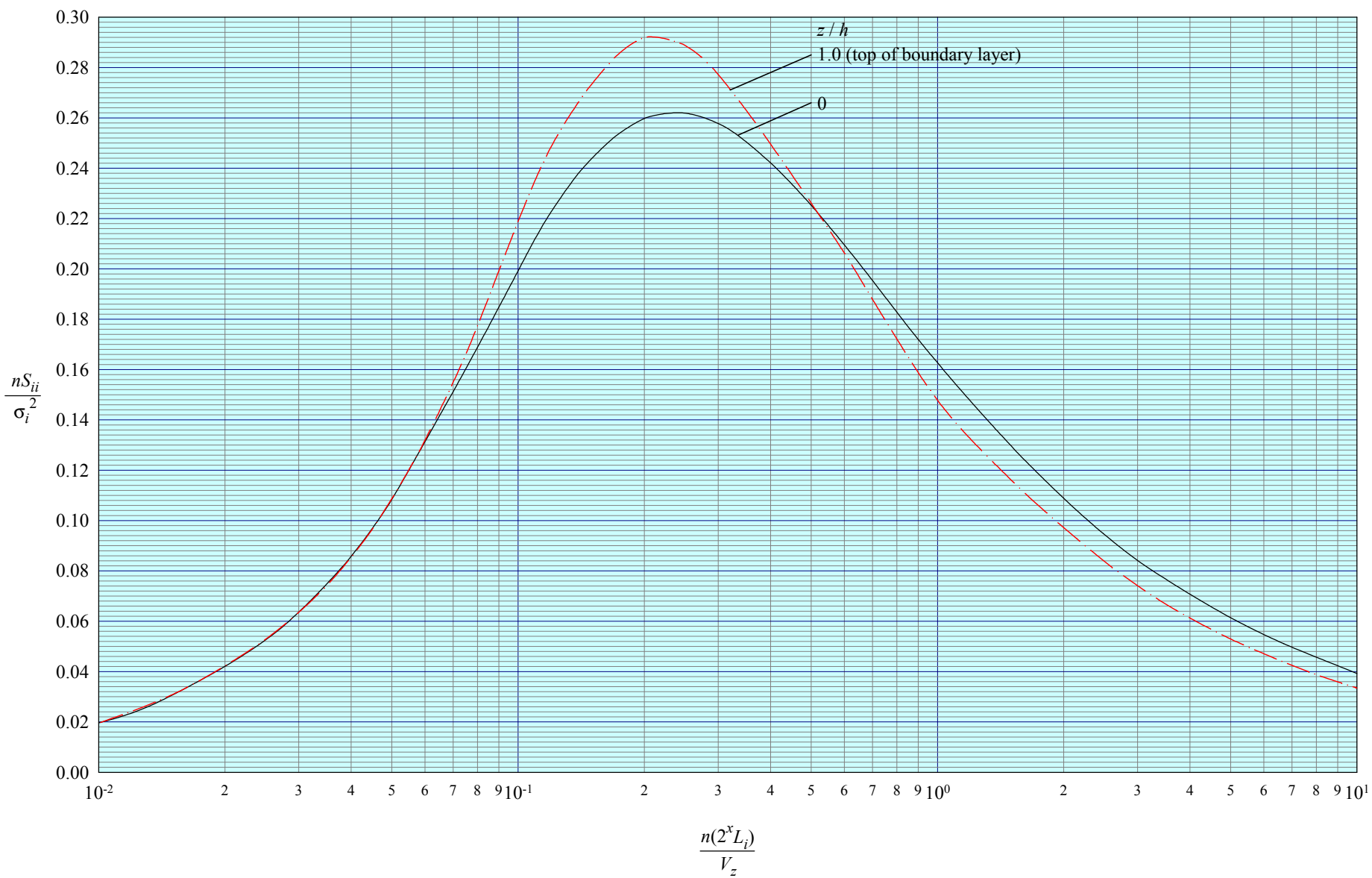


FIGURE B3 SPECTRAL DENSITY FUNCTION FOR $i = v$ - OR w -COMPONENT

KEEPING UP TO DATE

Whenever Items are revised, subscribers to the service automatically receive the material required to update the appropriate Volumes. If you are in any doubt as to whether or not your ESDU holding is up to date, please contact us.

Please address all technical engineering enquiries and suggestions to:

ESDU International plc	Tel:	020 7490 5151 (from the UK) +44 20 7490 5151 (from outside the UK)
	Fax:	020 7490 2701 (from the UK) +44 20 7490 2701 (from outside the UK)
	E-Mail:	esdu@esdu.com
	Website:	www.esdu.com

For users in the USA, please address all Customer Service and Support enquiries and suggestions to:

IHS Engineering Products and Global Engineering Documents	Tel:	1 800 525 7052 (toll free number)
	Fax:	1 303 397 2599
	Website:	www.ihs.com www.global.ihs.com

**Characteristics of atmospheric turbulence near the ground.
Part II: single point data for strong winds (neutral atmosphere)
ESDU 85020**

ISBN 0 85679 526-7, ISSN 0143-2702

Available as part of the ESDU Series on Wind Engineering. For information on all ESDU validated engineering data contact ESDU International plc, 27 Corsham Street, London N1 6UA.

Turbulence properties in the atmospheric wind are important in estimating wind loading effects. The applications range from aircraft response predictions to the estimation of peak loadings on ground-based structures.

ESDU 85020 (which supersedes ESDU 74031) is part of a series of Items providing a comprehensive set of turbulence characteristics in the atmospheric boundary layer for strong wind conditions (neutral atmosphere). This part deals with the properties of the longitudinal (u), lateral (v) and vertical (w) components of fluctuating wind speed measured at a single point in space. The properties covered are turbulence intensity, Reynolds stresses, probability density, spectral density and integral length scales of turbulence. The data are applicable up to a height of at least 300 m and for a range of surface roughnesses including terrain with upwind roughness changes.

The data are derived from models based on measurements from the most reliable sources and on similarity theory as applied to the atmospheric boundary layer. The result follows that the properties are dependent on the reference wind speed except in a layer close to the ground. The theoretical basis allows a rational extrapolation from measurements obtained at moderate wind speeds to the much higher design wind speed case when, in particular, much larger length scales are obtained except near ground level. Modified spectral equations are derived to account for anisotropic turbulence close to the ground.

A computer program ESDUpac A9232, described in ESDU 92032, can be used to generate intensities, length scales and spectral densities of the u , v and w components of turbulence.

© ESDU International plc, 2001

All rights are reserved. No part of any Data Item may be reprinted, reproduced, or transmitted in any form or by any means, optical, electronic or mechanical including photocopying, recording or by any information storage and retrieval system without permission from ESDU International plc in writing. Save for such permission all copyright and other intellectual property rights belong to ESDU International plc.